

INTRODUCTION

Little is known about the biogeochemical cycling and fate of marine toxins, particularly for that fraction of toxic compounds produced during bloom events that are not bioaccumulated and transferred through the food chain. This is the case for the marine toxin, domoic acid, which is produced by several *Pseudo-nitzschia* diatom species. Domoic acid is a potent glutamate agonist (Hampson and Manolo, 1998), and as such is toxic to marine invertebrates that graze on diatoms and other phytoplankton (Shaw et al., 1997; Windust, 1992). It has proven to be a threat to public health and some marine life in the areas where it is most prominent, particularly North American coastal waters. It was originally discovered in eastern Canada in 1987 as the causative agent in an episode of fatal human poisoning (Wright et al., 1989; Todd, 1993). It has been the cause of severe economic losses in the shellfish and crustacean harvesting industry of this area and off the Western coast of North America, and it has resulted in the death of many seabirds (Work et al., 1993; Sierra-Beltran et al., 1997) and mammals (Lefebvre et al., 2002; Scholin et al., 2000).

The environmental impact of domoic acid as a toxic compound capable of altering biochemical processes greatly depends upon its residence time and fate in natural waters. Although domoic acid may be degraded by bacterial processes within certain shellfish tissues (e.g., *Mytilus edulis*; Stewart et al., 1998), it has been found in the tissues of a wide variety of marine species, including both pelagic and benthic fish, shellfish, crustaceans, and marine mammals (Lefebvre et al., 2002; Bargu et al., 2003). A toxic bloom of *P. australis* in Monterey Bay, California in 2000 resulted in maximum cell

concentrations of greater than 2×10^6 cells L^{-1} , and dissolved domoic acid concentrations varying from undetectable to 130 nM (Doucette et al., 2002).

Virtually nothing is known regarding the biogeochemical cycling and ultimate fate of domoic acid once it is released into the water column. It is known that brief exposure (10-15 min) of domoic acid solutions to UV radiation (254 nm) in the laboratory yielded a series of three geometrical isomers which had been found earlier in extracts of the digestive glands of contaminated mussels (Wright et al., 1990). The presence of these photoisomers in the digestive glands of shellfish suggests this photochemical process may occur in ambient conditions in the water column. Studies have suggested the domoic acid isomers are less potent than domoic acid itself, whereas those isomers with Z configuration at the double bond closest to the ring (like domoic acid) have maximum potency (Hampson, 1992). In addition, exposure of domoic acid to artificial sunlight in seawater for 24 h yielded a group of less polar products believed to be decarboxylated derivatives of domoic acid (Campbell et al., in press).

Rue and Bruland (2001) recently demonstrated that domoic acid is an effective chelator for Cu(II) and Fe(III), both of which are bioactive trace metals of vital importance to a variety of biochemical processes occurring in natural waters. This is not completely unexpected since the carboxyl groups in domoic acid could act as electron donors in the chelation of such metal cations. Both Fe and Cu undergo a variety of light mediated redox reactions (involving Fe(II)/Fe(III) and Cu(I)/Cu(II) transformations) when complexed to organic ligands (Miller et al., 1995; Voelker et al., 2000). Therefore, the occurrence of chelated domoic acid complexes may be very significant to the ultimate fate of the toxin in natural waters. It is hypothesized that photochemical degradation and

trace metal chelation are thus important factors controlling the biogeochemical cycling and ultimate fate of domoic acid in natural waters.

Domoic acid-producing strains of *Pseudo-nitzschia* may have a competitive advantage over other species of phytoplankton that do not produce this toxin. Rue and Bruland (2001) speculated that complexation of Fe(III) and Cu(II) by domoic acid may provide *Pseudo-nitzschia* some competitive advantage in coastal waters in which it blooms. For example, Fe complexation by domoic acid may facilitate cellular uptake in Fe-limited waters in which *Pseudo-nitzschia* grows (Hutchins and Bruland, 2001; Maldonado et al., 2002). Copper complexation by domoic acid may serve to reduce concentrations of free hydrated Cu(II), which is widely recognized as a toxic form of Cu for marine phytoplankton (Sunda and Guillard, 1976; Brand et al., 1986; Moffett and Brand, 1996). Certain marine species, such as the cyanobacteria *Synechococcus*, are sensitive to free Cu(II) levels as low as 10^{-11} M (Brand et al., 1986). Moffett and Brand (1996) demonstrated that *Synechococcus* produces a strong ligand under Cu-stressed conditions in coastal waters, presumably as a detoxifying mechanism.

The observation of production of domoic acid photoisomers under UV radiation (254 nm) (Wright and Quilliam, 1995) raises several new and important questions regarding the environmental cycling and fate of domoic acid. The focus of the research described in this thesis is that of answering some of these important questions. For example, how efficient is ambient sunlight in degrading domoic acid to its photoisomers and decarboxylated products? What wavelengths of light are responsible for initiating these reactions, and by what mechanism does photodegradation of domoic acid proceed?

The effect of complexation of redox-active metals such as Fe(III) and Cu(II) on the photochemical degradation of domoic acid is also an important question. Organic complexes of these metals are photochemically reactive to various degrees as a result of electron transfer between metal and organic moieties (Finden et al., 1984; Waite and Morel, 1984; Bruland et al., 1991; Wells et al., 1991; Miller et al., 1995; Voelker et al., 2000). Results have demonstrated that Cu chelated to naturally occurring chromophoric dissolved organic matter significantly impacts its photodegradation in natural waters (Kieber et al., 2002) (Figure 1). Weaker Cu-organic complexes are relatively more reactive to photodegradation, suggesting that the strength of the complexes (e.g., as measured by conditional stability constants) is an important factor in determining photochemical reactivity (Voelker et al., 2000; Whitehead, via direct communication). It is therefore hypothesized that the demonstrated complexation of domoic acid and its photoisomers by redox-active trace metals such as Cu and Fe will influence the efficiency and products of the photodegradation process.

There are two main objectives of this research. The first is to determine if the photodegradation (and subsequent residence time) of domoic acid in natural waters is accelerated by photochemical processes. According to the first law of photochemistry, photons must be absorbed in order for a photochemical reaction to occur (Whitehead and de Mora, 2000). These photons may be absorbed by the analyte of interest (in this case, domoic acid) or they may be absorbed by some other species in the sample matrix. In a direct or primary photochemical process, photons are absorbed by the analyte of interest and a photochemical change is induced. Direct photochemical processes may also lead to the production of short-lived intermediates which are available to interact with the

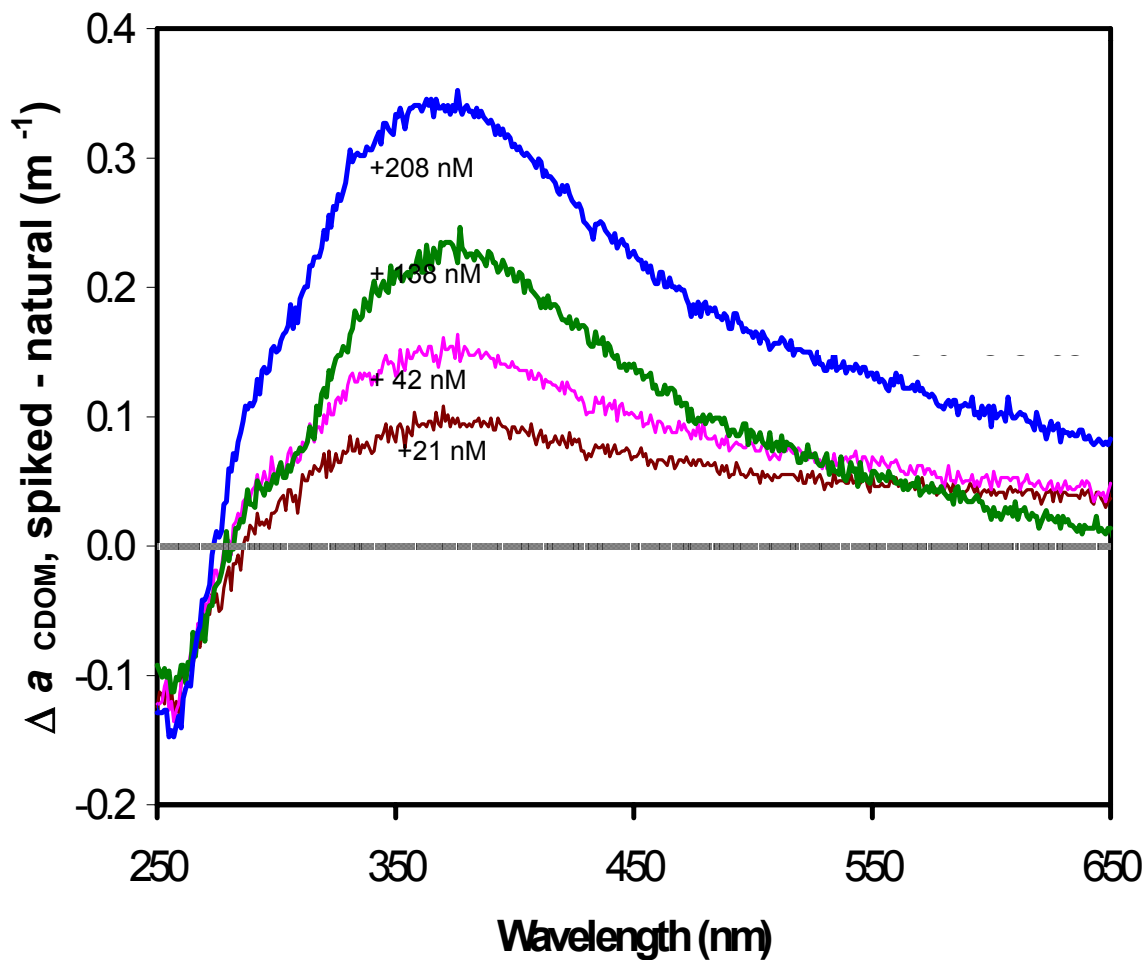


Figure 1: Effects of increasing Cu concentration on the degradation (as measured by loss of absorbance) of chromophoric organic material in estuarine water exposed to simulated sunlight. The results indicate that as Cu concentration increases there is a loss of absorbance (i.e., less degradation), presumably due to the formation of relatively unreactive strong Cu complexes (Whitehead, via direct communication).

analyte of interest to induce a photochemical change. For example, the irradiation of chromophoric dissolved organic matter leads to the production of hydroxyl radicals which can then interact with other compounds in the sample matrix to bring about photodegradation. These short-lived intermediates interact with the analyte of interest in an indirect or secondary photochemical reaction. After determining the type of photochemical reaction, if any, domoic acid undergoes, additional research was conducted to determine if the photodegradation of domoic acid is slowed or enhanced by the formation of trace metal chelates.

METHODS

Reagents and Standards

All chemicals were obtained from Fisher Scientific, Sigma-Aldrich Chemical, or VWR International and were HPLC grade unless otherwise stated. Solid domoic acid (99% purity) was purchased from VWR International and used to make all domoic acid samples. Domoic acid standard reference material was purchased from the Canada National Research Council and used to make calibration standards. A Milli-Q Plus Ultra-pure water system (Millipore, Bedford, MA) provided deionized water ($\geq 18.2 \text{ M}\Omega \text{ cm}^{-1}$) for the dilution of the domoic acid standard reference material along with all other reagents and standards unless otherwise noted.

Domoic Acid in Wrightsville Beach Seawater

A 32 μM primary stock of domoic acid was made by dissolving solid domoic acid in 10% acetonitrile in deionized water. The stock solution was stored in the dark at 4°C and was used for domoic acid photochemical experiments. Samples for individual experiments were made by diluting domoic acid primary stock in 0.2 μm filtered

Wrightsville Beach seawater (WBSW) to a final concentration ranging from 80-100 nM. Wrightsville Beach seawater (salinity ~32-34) was collected from the north end of Wrightsville Beach, North Carolina (34.208N, 77.796W) in an acid cleaned 10 L fluorinated polyethylene (FLPE) carboy and stored in the dark at 5°C until filtered to prevent bacterial growth. Clean WBSW was collected every 1-2 weeks in order to prevent contamination.

Controlled photolysis experiments were performed to determine the rate of photodegradation of domoic acid in seawater. The samples were distributed into eleven 10-cm long quartz spectrophotometric cells. Ten cells were placed in a circular carrier and submerged into a controlled temperature water bath. Samples were irradiated using a solar simulator (Spectral Energy solar simulator LH lamp housing with a 1000 watt Xe arc lamp) equipped with a sun lens diffuser and an AM1 filter to remove wavelengths not found in the solar spectrum, while the eleventh cell was placed in a dark cabinet at room temperature. Light measurements at each cell location were made with an Ocean Optics SD2000 spectrophotometer connected to a fiber optic cable terminated with a CC-UV cosine collector. In order to ensure that all cells received the same intensity of radiation, the cell holder was rotated 90° every half hour. The domoic acid sample was irradiated under simulated sunlight for a total of 10 h. Two cells were removed from the solar simulator every 2 h in order to analyze duplicate light exposed samples. Duplicate 400 µL aliquots were also removed from the dark control every 2 h for analysis.

Domoic Acid Analysis

All light exposed and dark control domoic acid samples were derivatized with 9-flourenylmethylchloroformate (FMOC-Cl) according to a modified version of the method

described by Pocklington et al. (1989). A solution of FMOC-Cl was prepared by diluting 1 g of FMOC-Cl in 250 mL of acetonitrile. The solution was distributed into 2 mL glass vials and blown with nitrogen gas before being capped with a Teflon-lined cap and stored in a desiccator at -20°C. Vials were removed from the freezer as needed, and any unused portion was disposed of.

A 1 M borate buffer solution was prepared by dissolving 6.18 g of ortho-boric acid in 95 mL of deionized water. The pH of the solution was adjusted to 6.2 with a solution of 5 M sodium hydroxide. The volume of the buffer was then brought to 100 mL with deionized water. The borate buffer was filtered through a 0.2 µm filter on a weekly basis in order to remove particles that may have precipitated out of solution.

Domoic acid samples were derivatized by combining 400 µL of sample, 40 µL of borate buffer, and 500 µL of FMOC-Cl in a 3.5 mL glass test tube. The sample was shaken with a vortex mixer for 45 seconds. Ethyl acetate (1 mL) was added to the sample mixture to extract the excess FMOC-Cl reagent, after which the sample was vortex-mixed a second time for 45 seconds, and the top organic layer was removed with a disposable Pasteur pipet. An additional aliquot of ethyl acetate (1 mL) was added to the sample and vortex-mixed for another 20 seconds followed by removal of the organic layer. This was repeated for a third and final time, and the bottom layer was removed with a clean Pasteur pipet and placed in a small sample vial containing a glass micro-insert. Once derivatized, all samples were refrigerated until analyzed by HPLC. Storage experiments done by Pocklington et al. (1989) indicate derivatized solutions appear to be stable for at least one week in the light at room temperature. Domoic acid samples were stored in the dark at 4°C for no more than 1-2 weeks before being analyzed.

High Performance Liquid Chromatography

A Hewlett-Packard series 1100 high performance liquid chromatograph (HPLC) was used to analyze the domoic acid samples. The HPLC was outfitted with a variable volume (1-25 μL) injector and auto sampler, heated column compartment, and Agilent Technologies data system. It was coupled to an external Shimadzu RF-551 PC spectrofluorometric detector set at an excitation wavelength of 264 nm and emission wavelength of 313 nm. A 25 cm x 4.6 mm I.D. reverse phase C_{18} column packed with 5 μm particles (Vydac 201TP column) maintained at a temperature of 55°C was used to separate the domoic acid derivatives. The mobile phase consisted of aqueous acetonitrile with 0.1% trifluoroacetic acid (TFA) at a flow rate of 1.0 mL min^{-1} . Gradient elution was programmed from 30% acetonitrile with 0.1% TFA to 70% over 15 min, followed by an increase to 100% acetonitrile with 0.1% TFA over the next 2 min, which was maintained for 7 min before cycling back to 30% acetonitrile with 0.1% TFA. The total analysis time was 35 min, and the injection volume was 10 μL .

A 2.9 μM stock solution of domoic acid standard was prepared by diluting the standard reference material in deionized water and was subsequently stored in the dark at 8°C. Domoic acid calibration solutions were prepared by diluting the standard stock solution in deionized water to final concentrations of 10, 25, 50, 100, and 150 nM. The calibration solutions were then derivatized with FMOC-Cl and stored in the dark at 8°C until analyzed on the HPLC. A new calibration curve (Figure 2) was created for each set of samples run on the HPLC. One hundred nM standards were run between several domoic acid samples in order to calibrate for instrument drift. The relative standard deviation was 1.8%, and the detection limit was less than 10 nM. Blank samples (sample

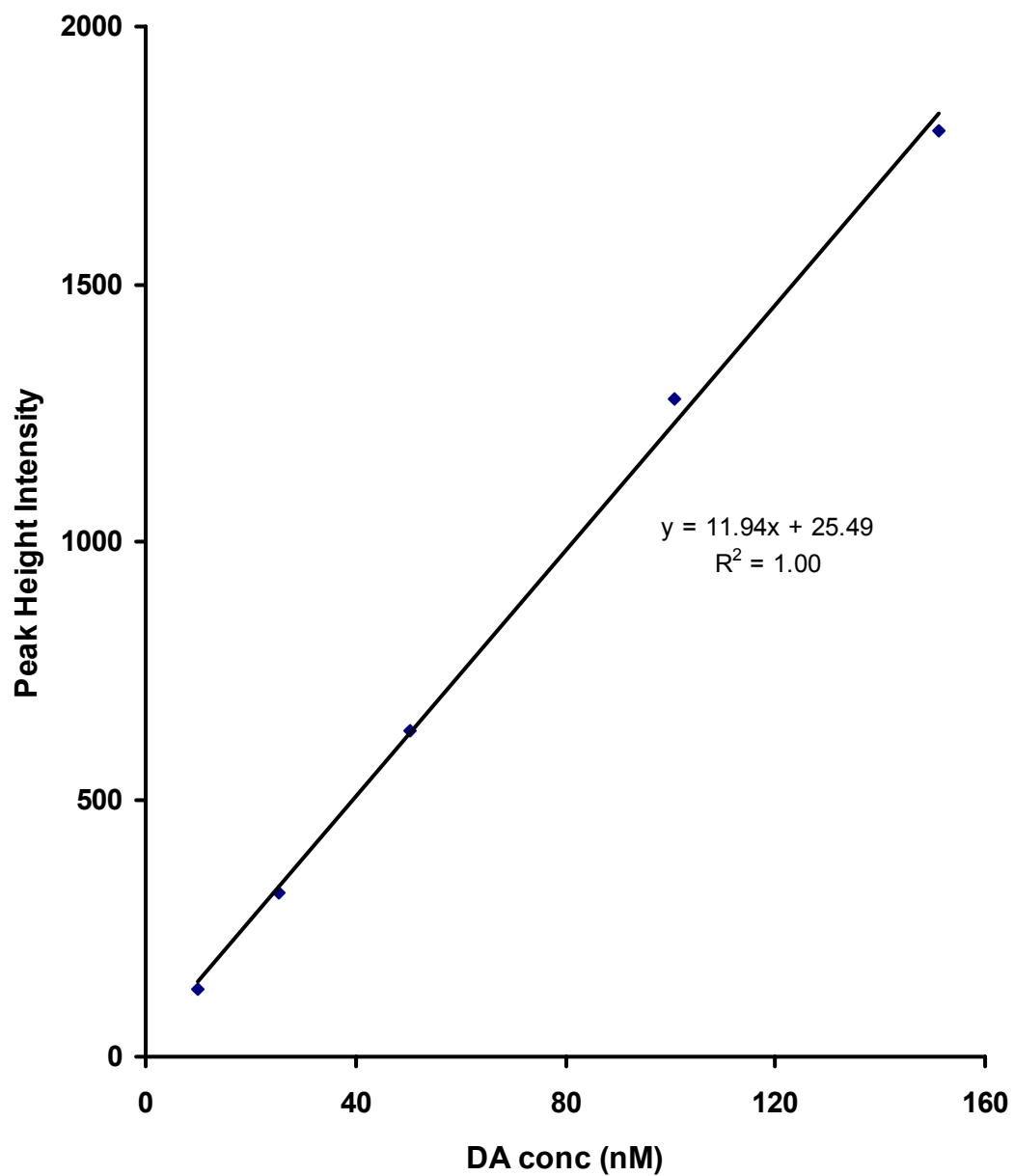


Figure 2: Peak height as a function of concentration of added domoic acid in a typical HPLC calibration curve.

matrix minus domoic acid) contained non-detectable levels of domoic acid.

Additional Photolysis Experiments

To determine the effect of sample matrix on the photodegradation of domoic acid, a series of different additions were made to the WBSW samples. To determine the effect of dissolved organic carbon (DOC), ionic strength, and pH on the photodegradation of domoic acid, a domoic acid sample was made up in deionized water rather than WBSW. The sample was distributed into eleven 10-cm long quartz spectrophotometric cells. Samples were irradiated in a fashion analogous to the WBSW experiments, derivatized according to the method described above, and analyzed by HPLC. In addition to this experiment, another experiment was performed in which humic material (20 mg L^{-1}) was added to the domoic acid sample in deionized water. The sample was distributed into eleven 10-cm long quartz cells and irradiated under simulated sunlight in a fashion analogous to the WBSW experiments. The samples were then derivatized and analyzed via HPLC.

The effect of oxygen and reactive oxygen species on the photodegradation of domoic acid was determined by deoxygenating a domoic acid sample with nitrogen gas. Domoic acid was added to WBSW to a final concentration of 83 nM. The sample was placed in a nitrogen-filled glove bag and bubbled with nitrogen gas for a total of 4 h. The sample sat overnight in the dark in the nitrogen atmosphere. The deoxygenated sample was distributed into eleven 10-cm long quartz cells, and the cells were capped inside of the nitrogen-filled glove bag. The samples were then irradiated in a fashion analogous to the WBSW samples, FMOCCl derivatized, and analyzed by HPLC.

The effect of hydroxyl radicals was determined by spiking a domoic acid sample with a hydroxyl scavenger, methanol (Mopper et al., 1990). Domoic acid was added to filtered WBSW to a final concentration of 92 nM. The sample was then spiked with 40 mM methanol and distributed into eleven 10-cm long quartz cells. The sample was irradiated in a solar simulator in a fashion analogous to the WBSW without added methanol experiments. The samples were then derivatized with FMOC-Cl and analyzed by HPLC.

A series of temperature experiments were conducted to determine the effects of temperature on the photodegradation of domoic acid and to determine the activation energy of photodegradation. Domoic acid samples were made up in WBSW to a final concentration of 80-100 nM. The samples were distributed into eleven 10-cm long quartz spectrophotometric cells and irradiated in a fashion analogous to the WBSW samples; however, the temperature of the water bath was adjusted to 5°C, 10°C, 15°C, and 20°C. Control samples were kept in a dark cabinet in a cold room set to the appropriate temperature.

An additional experiment was performed where a domoic acid sample (72 nM) in WBSW was irradiated under visible light (400-700 nm) only. Ultraviolet radiation (280-400 nm) was blocked with a cut-off filter equipped to eliminate wavelengths lower than 400 nm.

Trace Metal Experiments

Iron(III) and Cu(II) were added to domoic acid samples to determine the effect of trace metal chelates on the photodegradation of domoic acid in seawater. In preparation for these trace metal experiments, all glassware, including quartz cells and pipet tips,

were soaked in 10% HCl for 24 hours, rinsed with deionized water, and placed in a class 100 clean bench to dry completely. Sample preparation for the Fe(III) and Cu(II) experiments along with the FMOC-Cl derivatization procedure for these experiments were performed in a class 100 clean room to minimize contamination.

A secondary stock of Fe(III) was prepared by adding 500 μL of 1000 ppm ferric nitrate standard (Fisher Scientific) to 4.5 mL of deionized water. A sample (500 mL) of domoic acid (100 nM) in 0.2 μm filtered WBSW was spiked with the secondary Fe(III) stock to a final concentration of 107 nM. The Fe(III)-spiked domoic acid sample sat overnight at room temperature in the dark to allow complexation to occur. The sample was distributed into eleven 10-cm long quartz cells and irradiated in a fashion analogous to the WBSW with no added Fe samples. This experiment was repeated a total of four times so that an average rate constant of photodegradation could be quantified. Total dissolved Fe concentrations were determined by the ferrozine method modified from Stookey (1970). Absorbance measurements were made using a 1 m (Ocean Optics) or a 5 m (World Precision Instruments) liquid waveguide capillary cell (LWCC) attached to an Ocean Optics Inc. SD2000 spectrophotometer and an Analytical Instrument Systems Inc. Model DT 1000 CE UV/Vis Light Source (Hardison, 2002).

Four trials involving addition of Cu(II) to domoic acid samples were also conducted by adding 2.5 mL of a 20.048 μM Cu(II) standard (pH \sim 4) to a sample (500 mL) of domoic acid (100 nM) in WBSW to a final concentration of 100 nM Cu(II). The pH of the solution was adjusted to that of seawater (\sim 8.0) using high-purity NH_4OH (Fisher Optima). The Cu(II)-spiked solution sat overnight at room temperature in the dark so that complexation could occur. The sample was then distributed into eleven

10-cm long quartz cells and irradiated in a fashion analogous to the WBSW without added metals experiments. Total Cu concentrations were determined by the bathocuproine method modified from Clesceri et al. (1989) and were spectrophotometrically determined with a Spectronic 1001 Plus (10 cm pathlength).

RESULTS

A series of four controlled photolysis experiments were conducted to determine rates of domoic acid photodegradation in natural waters. Each experiment consisted of the addition of domoic acid to 0.2 μm filtered Wrightsville Beach seawater (WBSW) to a final concentration ranging from 80-100 nM. Duplicate light-exposed and dark control samples were taken every 2 h. All samples were derivatized with FMOC-Cl and analyzed by HPLC according to the method described by Pocklington et al. (1989). Over the ten hour irradiation period, there was a significant loss of domoic acid in the light exposed cells with concentrations decreasing on average from 84 to 18 nM (Figure 3). No loss of domoic acid was observed in the dark controls.

Photodegradation of domoic acid yielded three distinct products. HPLC analysis of the sample at $T = 0$ h showed domoic acid ($RT = 9.5$ min) as the only substance present in the sample with the exception of a few reagent peaks (Figure 4a). After irradiation, the peak height of domoic acid clearly diminished in the light exposed samples and three photoproducts formed (Figure 4b). Two of these photoproducts eluted from the column prior to domoic acid ($RT = 8.7$ min and 9 min) whereas a third eluted later ($RT = 10$ min). These photoproducts have been identified to be the three geometrical isomers of domoic acid discovered by Wright et al. (1990) (Figure 5). There was no loss of domoic acid in the dark control samples at $T=10$ hours (Figure 4c).

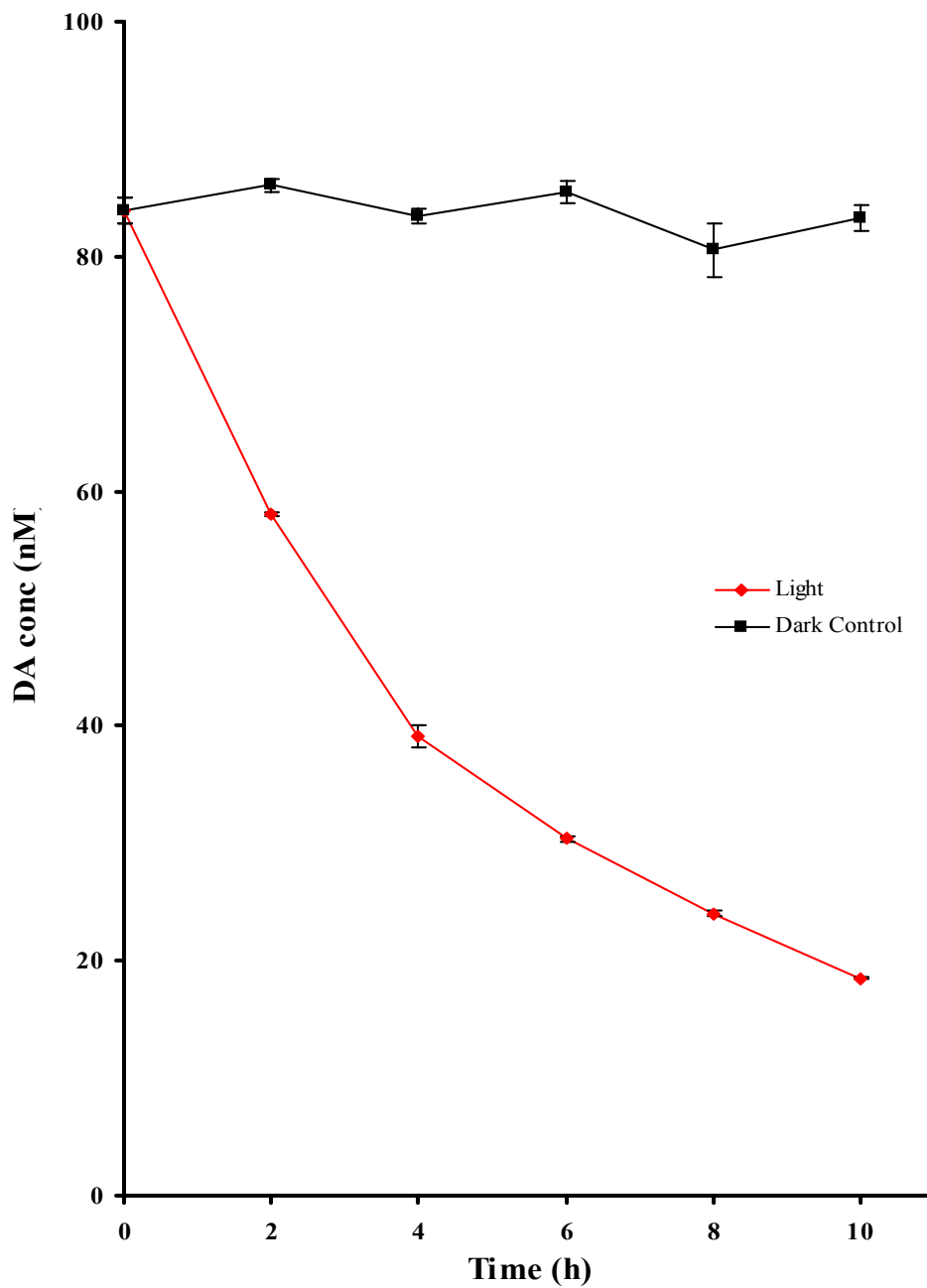


Figure 3: Concentration of domoic acid (nM) in light exposed and dark control samples as a function of irradiation time (h). Error bars represent the range (n = 2), while the absence of error bars signifies the range is smaller than the symbol. Salinity 34; pH 8.1.

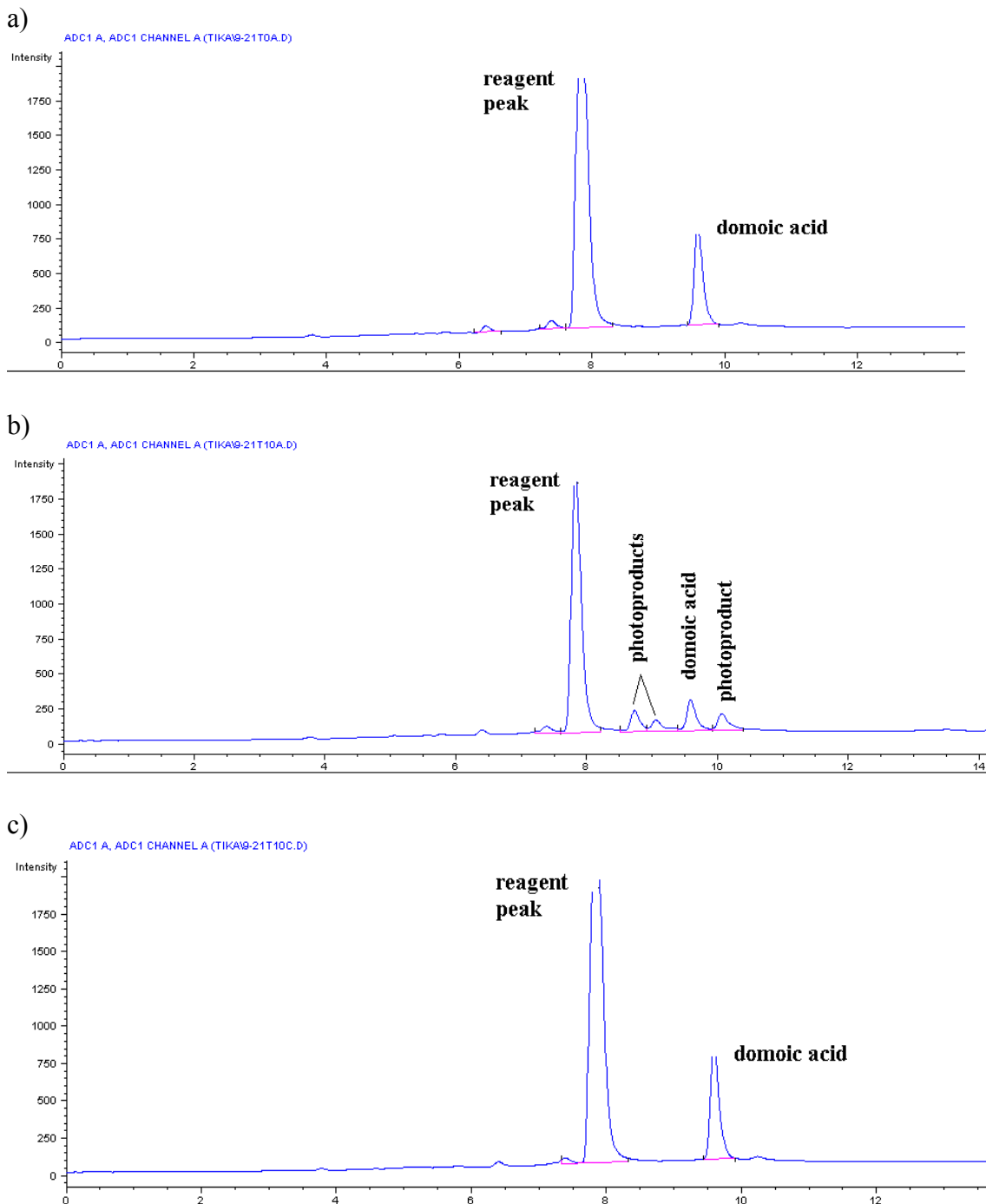


Figure 4: HPLC traces of Fmoc-derivitized domoic acid samples. a) T = 0 hours. b) light exposed sample (T = 10 h). c) dark control sample (T = 10 h). Domoic acid has a retention time of 9.5 minutes while the domoic acid photoproducts have retention times of approximately 8.5, 9.0, and 10.0 minutes. Salinity 34; pH 8.1.

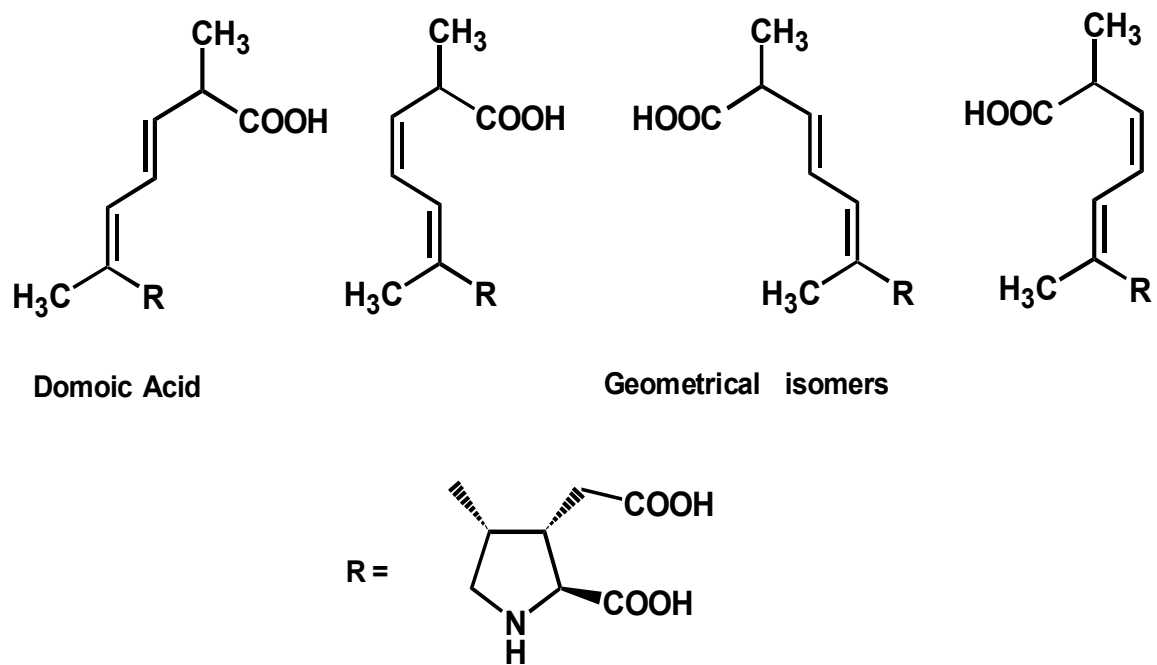


Figure 5: Domoic acid and its geometrical isomers (Wright et al., 1990)

The loss of domoic acid was plotted as a first order reaction in order to determine the rate of photodegradation (Figure 6). The calculated first order rate constant of domoic acid photodegradation is 0.15 h^{-1} . This value was normalized to the average light intensity of the solar simulator by taking the product of the calculated rate constant and the average light intensity divided by the light intensity for that specific experiment. After normalizing this value to the average light intensity of the solar simulator, the first order rate constant is 0.15 h^{-1} . The average normalized rate constant of domoic acid photodegradation in WBSW at 24°C is $0.15 \pm 0.01 \text{ h}^{-1}$ ($n = 4$). Values for the normalized rate constants of each individual photolysis experiment are shown in Table 1.

Domoic Acid in Deionized Water

To determine the effects of sample matrix on the rate of photodegradation of domoic acid in seawater, an additional photolysis experiment was conducted by spiking deionized water (Millipore Milli-Q; $\geq 18.2 \text{ M}\Omega \text{ cm}^{-1}$; $\text{pH} = 5.1$) with domoic acid and irradiating it under simulated sunlight for 10 h at 25°C , similar to the WBSW experiments presented in Table 1. The resulting rate constant in deionized water normalized to the light intensity is 0.16 h^{-1} (Figure 7), which is statistically equivalent (t-test, 95% confidence level) to the WBSW photodegradation rate constant. These results confirmed a recent study by Bates et al. (2003) who that found there was no significant difference in the photolytic loss of domoic acid regardless of the sample matrix. Losses of 36% and 41% occurred in deionized water and seawater, respectively. This suggests that DOC, ionic strength, and pH did not have an effect on the rate of photodegradation of domoic acid and that the photodegradation of domoic acid most likely proceeds via a direct photoprocess.

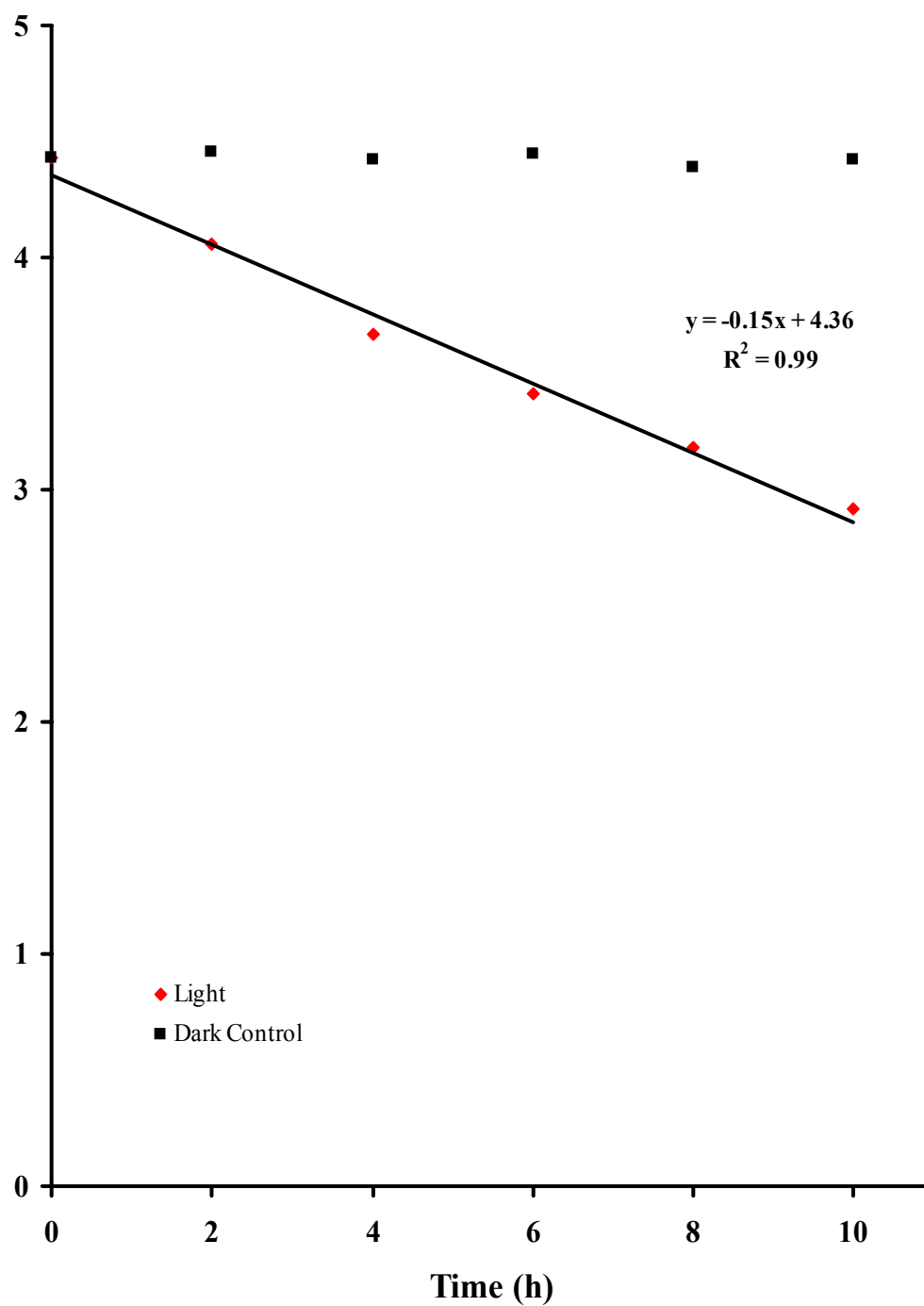


Figure 6: Natural logarithm of domoic acid concentration as a function of irradiation time (h). The line in the light exposed samples represents a best fit linear regression to the data. Salinity 34; pH 8.1.

Table 1: Rate constants of domoic acid in Wrightsville Beach seawater. All samples were irradiated for 10 hours under simulated sunlight at room temperature.

Trial	Salinity	pH	First Order Rate Constant normalized to average light intensity (h⁻¹)
1	34	8.0	0.15
2	34	8.1	0.15
3	34	8.1	0.14
4	34	8.1	0.14
Average			0.15 ± 0.01

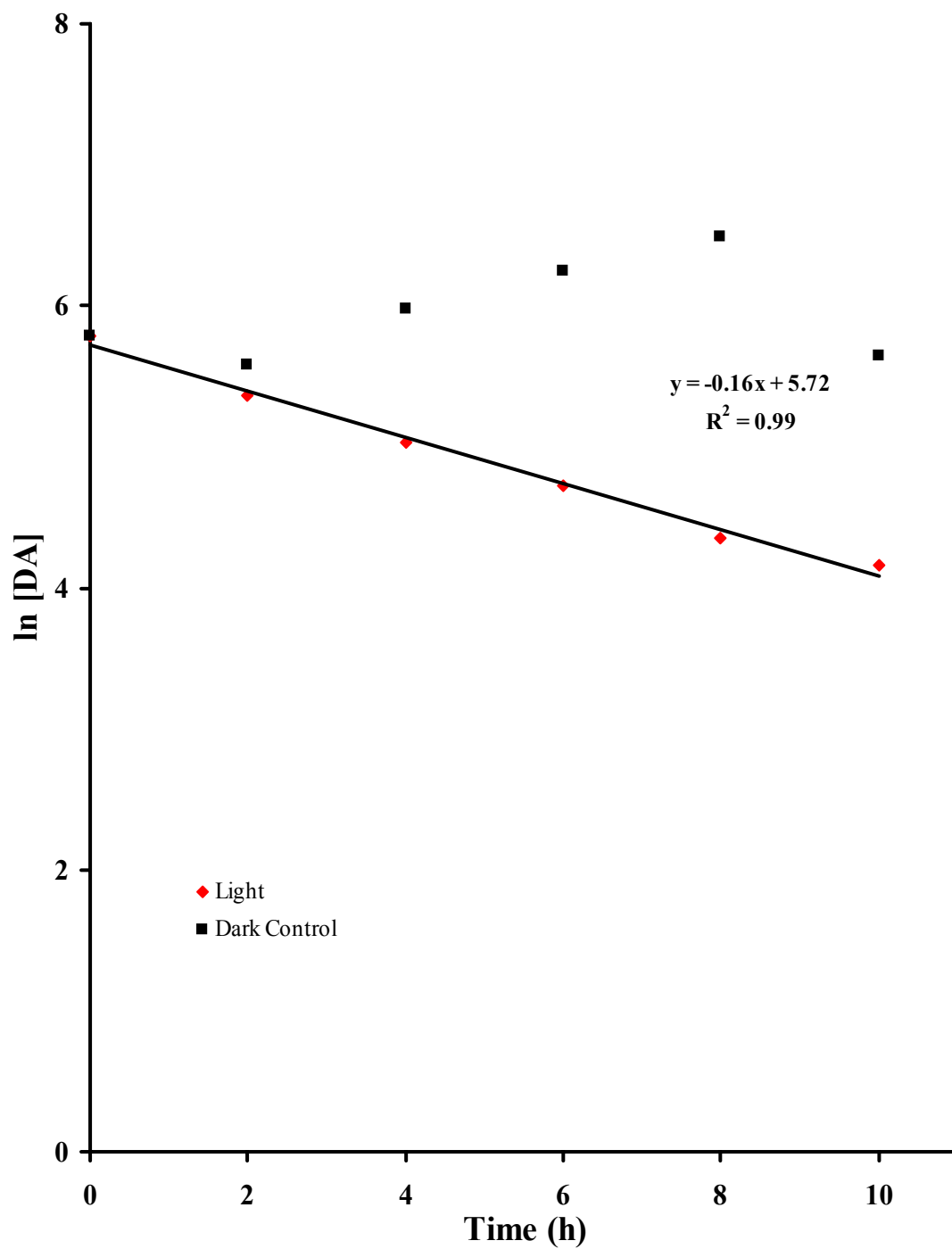


Figure 7: Natural logarithm of domoic acid concentration as a function of irradiation time (h) in deionized water. The line in the light exposed samples represents a best fit linear regression to the data. Salinity 0; pH 5.1.

Effect of Trace Metals on Domoic Acid Photodegradation

An additional photochemical experiment was performed to determine the effects of naturally-occurring concentrations of trace metals on the photodegradation of domoic acid in seawater. Sargasso seawater was treated with Chelex-100 resin to remove trace metals and subsequently UV-irradiated (1200 W mercury vapor lamp; Ace Glass) to destroy organic material. Domoic acid was added to the treated WBSW to a final concentration of 100 nM and irradiated under simulated sunlight for 10 h. The resulting normalized first order rate constant (Figure 8) was 0.15 h^{-1} and was statistically equivalent (t-test; 95% confidence level) to the first order rate constant of domoic acid in untreated WBSW.

A separate series of photolysis experiments were conducted in the presence of Cu(II) and Fe(III) (4 trials each) to determine the effect of redox-active trace metals on the photodegradation rates of domoic acid (Figure 9). Both metals were added to WBSW in a 1:1 ratio with domoic acid (ca. 100 nM each). The average normalized first order rate constant for domoic acid in the presence of Fe(III) was $0.14 \pm 0.01 \text{ h}^{-1}$ ($n = 4$), whereas that for domoic acid in the presence of Cu(II) was $0.15 \pm 0.01 \text{ h}^{-1}$ ($n = 4$). These values are not statistically different (t test, 95% confidence level) compared to the

photodegradation rates in WBSW with no added metals. This indicates that Fe(III) and Cu(II) do not significantly impact the photodegradation of domoic acid in seawater, and again are consistent with the results of Bates et al. (2003). When a sample of domoic acid in artificial seawater was spiked with iron, they also found no significant increase in the loss of domoic acid upon irradiation of the sample. With added iron, they found a 48% decrease in the concentration of domoic acid whereas a 44% decrease in

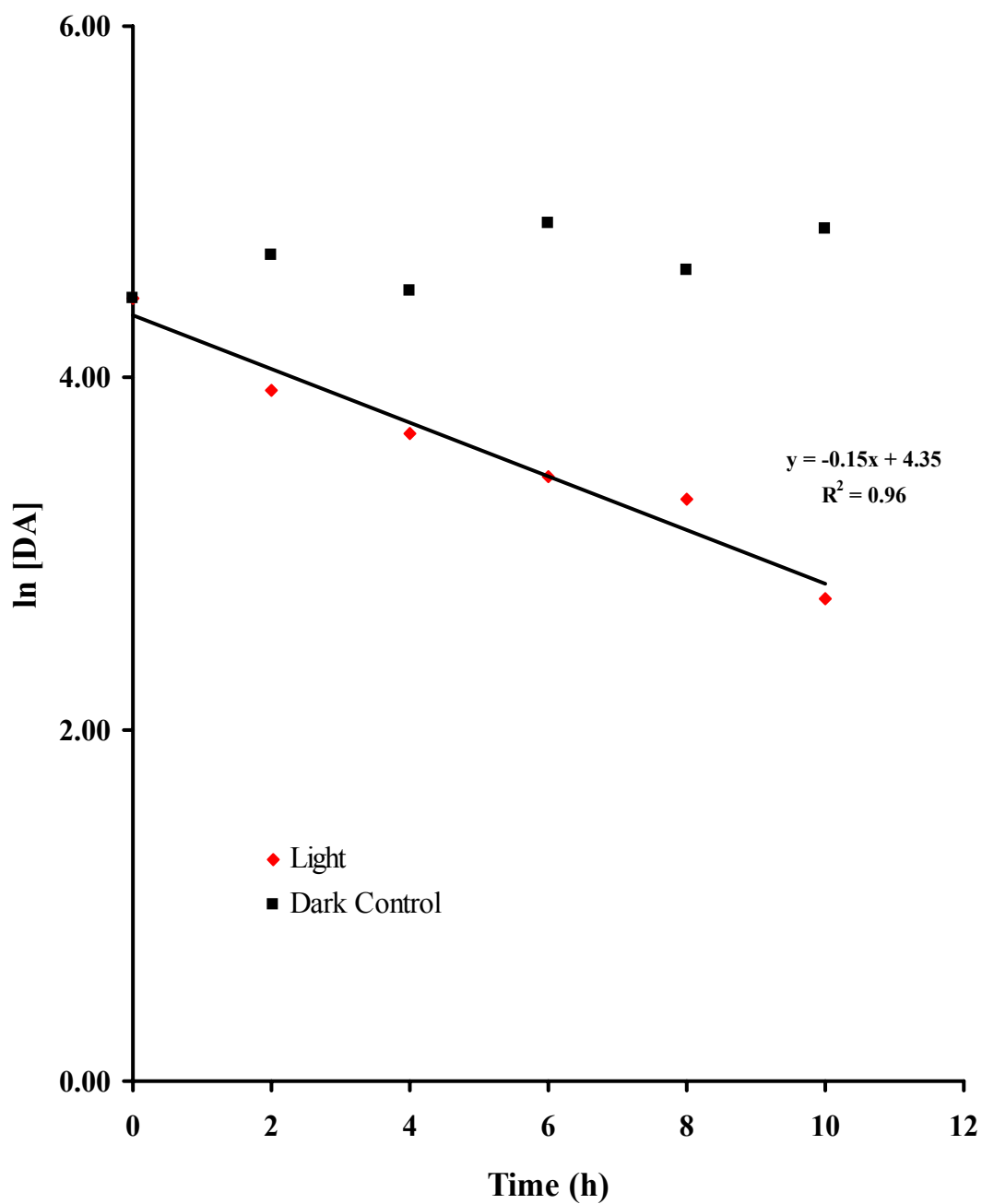


Figure 8: Natural logarithm of domoic acid concentration (nM) as a function of irradiation time (h). The line in the light exposed sample represents a best fit linear regression to the data. Domoic acid sample was made up in trace metal clean Sargasso seawater (treated with chelex-100 resin and subsequently UV irradiated). Salinity = 12; pH = 6.52.

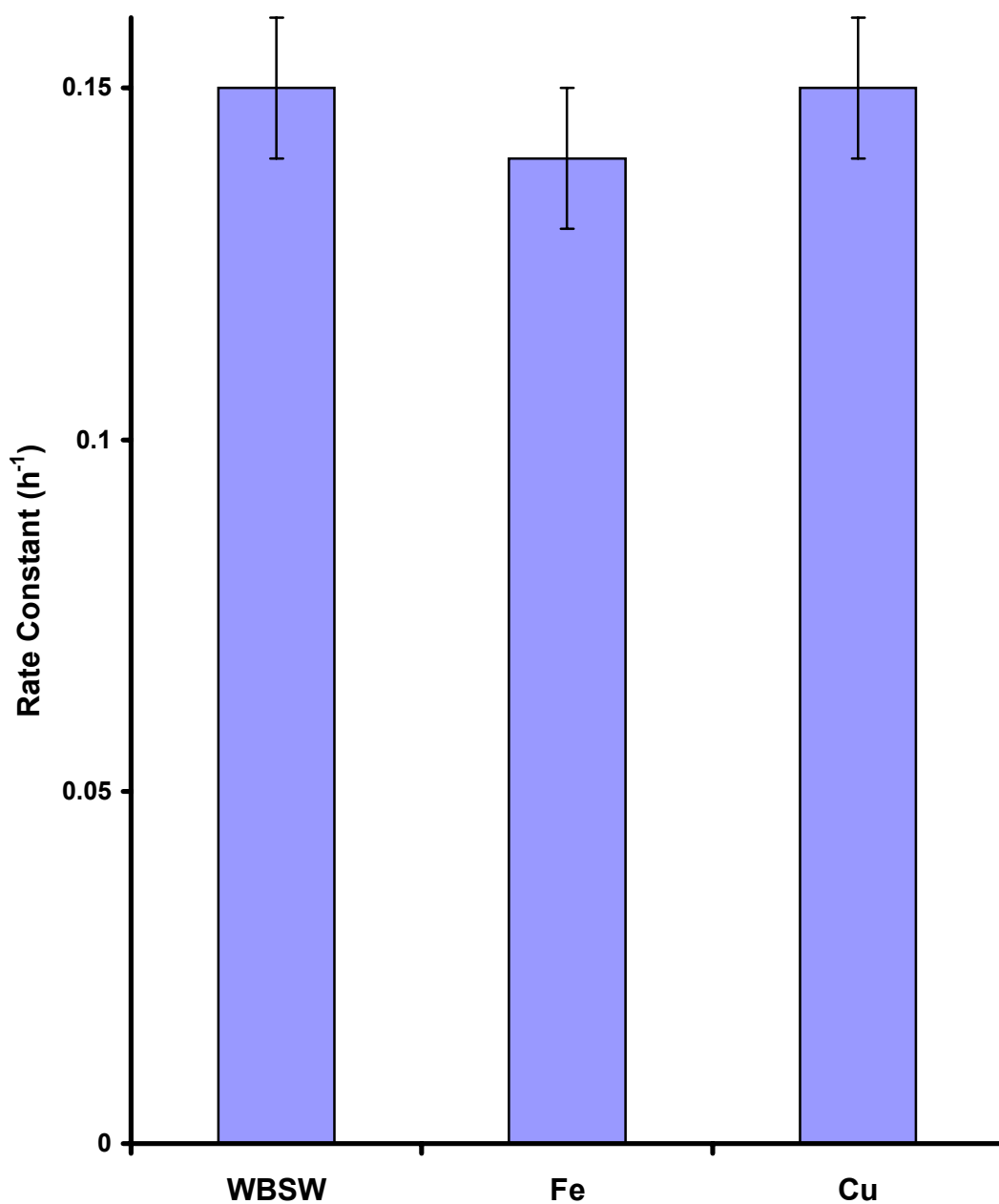


Figure 9: First order rate constant of domoic acid photo-degradation in Wrightsville Beach seawater (WBSW) with added Fe(III) and Cu(II) to a final concentration of 100 nM. Error bars represent the standard deviation ($n = 5$).

domoic acid concentration occurred with no added iron. These results imply that iron does not impact the rate of domoic acid photodegradation in seawater.

Effect of Sample Matrix on Domoic Acid-Fe(III) Complex

Experiments were performed in which domoic acid was added to deionized water (pH = 4.8) and spiked to a final concentration of 100 nM Fe(III) to determine the effects of sample matrix on the photolysis of the domoic acid iron complex. Addition of Fe(III) to domoic acid in deionized water resulted in a dramatic increase in the rate of photodegradation of domoic acid (normalized 1st order rate constant = 0.23 h⁻¹) relative to deionized water with no added Fe or WBSW with or without added Fe (Figure 10).

These experiments confirmed the results of Bates et al. (2003), who found that domoic acid in the presence of Fe(III) was nearly completely degraded in deionized water, but only 36% degraded in deionized water without Fe(III) added. The results may be explained by looking at the speciation of Fe(III) in seawater versus deionized water. The predominant forms of Fe(III) in seawater at a pH of 8 are Fe(OH)₃, which is insoluble, and Fe(OH)₄⁻, which is available to complex with ligands in the solution (Millero, 1996). Fe(OH)₂⁺ and FeOH²⁺ are the predominant forms of Fe(III) in deionized water at a pH of 5 (Stumm and Morgan, 1996). These forms of Fe(III) are available to complex with ligands in solutions, however, there are no ligands present in deionized water. Therefore, when domoic acid was added to deionized water in the presence of Fe(III), the dissolved Fe(III) complexes were available to complex with domoic acid whereas in seawater, there were many other competing ligands. Further studies will need to be conducted to determine exactly why the photodegradation of domoic acid in deionized water increased dramatically in the presence of Fe(III).

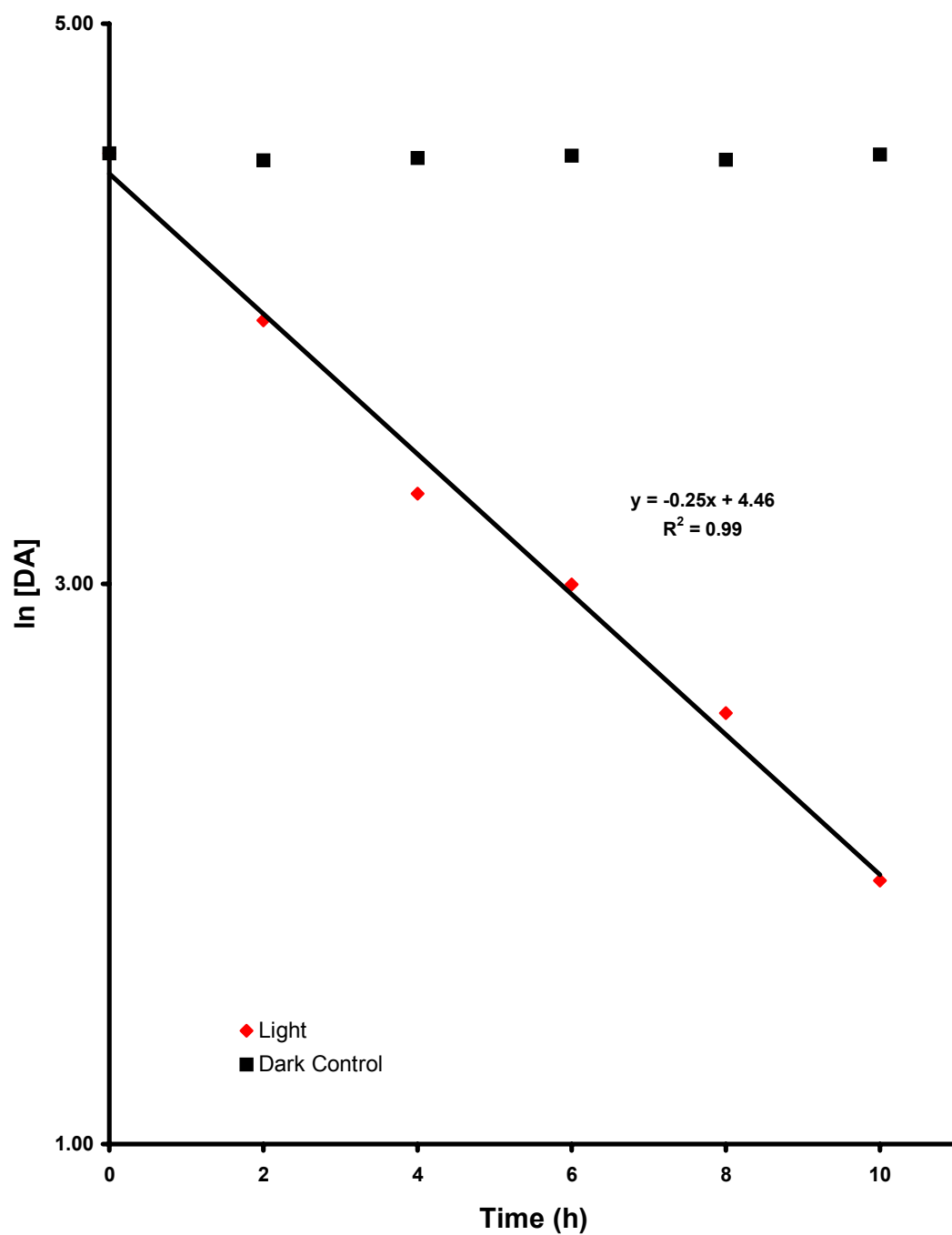


Figure 10: Natural logarithm of the domoic acid concentration as a function of irradiation time (h). Sample consisted of domoic acid in deionized water with added Fe(III) (ca. 100 nM). Salinity = 0; pH = 4.76.

Effect of pH on Photodegradation of Domoic Acid

A series of experiments were conducted in order to determine the effect of pH on the photodegradation of domoic acid in WBSW. Domoic acid was added to WBSW to a final concentration ranging from 80-100 nM and spiked with 107 nM Fe(III). The pH of the sample was then adjusted to 4, 5, 6, or 7 with HCl (Fisher Optima). Each sample was irradiated in the solar simulator for 10 h at 25°C. The results indicate that pH did not have an effect on the rate of photodegradation of domoic acid (Figure 11). An additional pH experiment was conducted in which the pH of WBSW was adjusted to pH ~4 prior to the addition of domoic acid and Fe(III). This method took into consideration the formation of colloidal suspensions that may occur with the addition of Fe(III) to the sample. Addition of domoic acid and Fe(III) after the pH adjustment did not alter the rate of photodegradation suggesting the order of reagent addition is not important.

DISCUSSION

Upon exposure to simulated sunlight, domoic acid photodegraded to a series of three geometrical isomers, along with other photoproducts in natural seawater. Following this observation, a series of photochemical experiments were conducted to explore the mechanism of domoic acid photodegradation in natural waters. The role of hydroxyl radicals ($\cdot\text{OH}$) was assessed by addition of the $\cdot\text{OH}$ scavenger, methanol, prior to irradiation. Hydroxyl radicals are produced upon irradiation of seawater due to the photolysis of species such as chromophoric dissolved organic matter (CDOM), NO_3^- , NO_2^- , and H_2O_2 (Mopper and Zhou, 1990). Once generated, they can interact with and transmit excitation energy to domoic acid. To examine this possibility, domoic acid was added to WBSW to a final concentration of 92 nM in the presence of MeOH (ca. 40 mM)

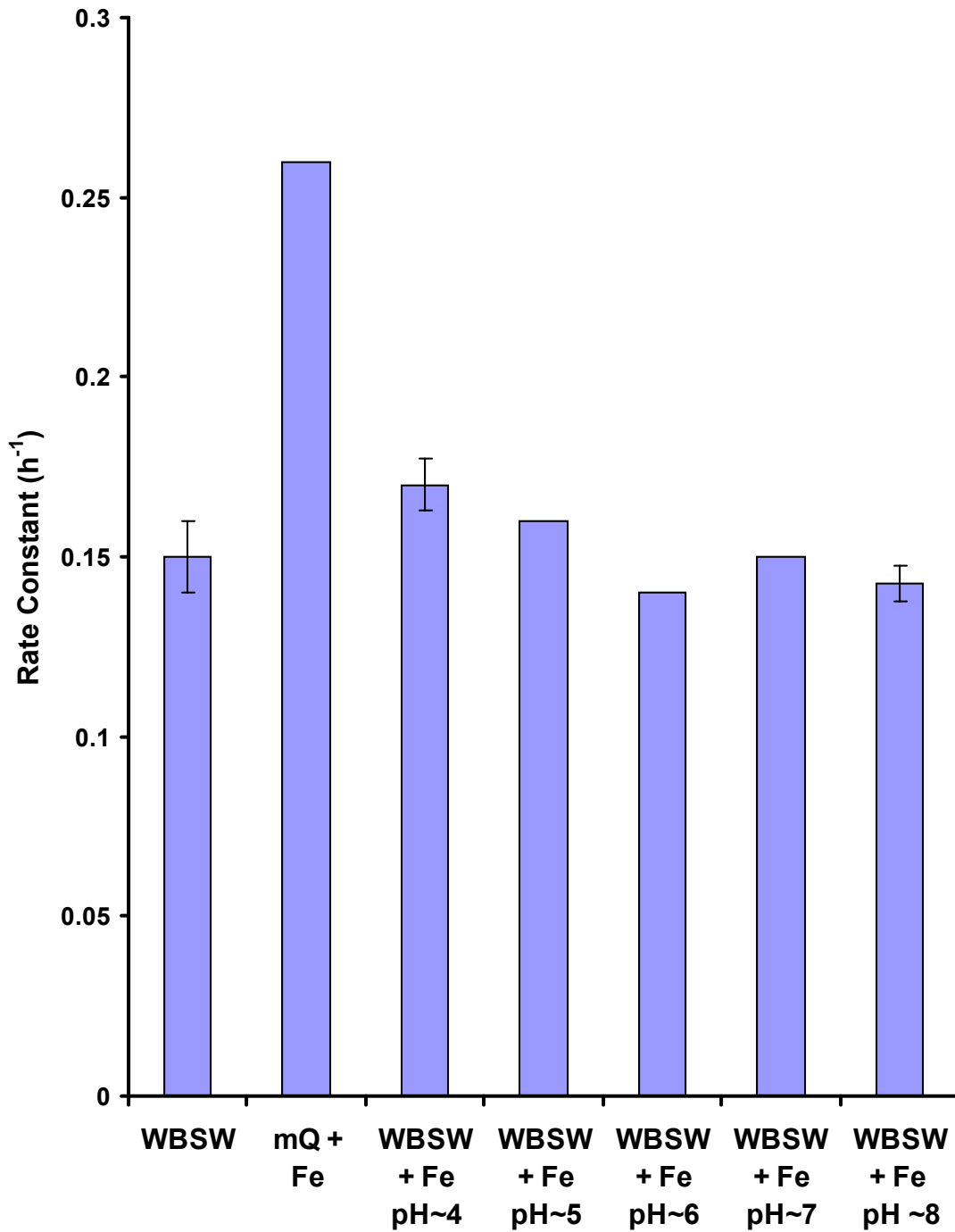


Figure 11: First order rate constants of domoic acid in Wrightsville Beach seawater (WBSW) at varying pH values in deionized water in the presence of 107 nM Fe(III). No error bars indicate $n = 1$.

The domoic acid concentration decreased with irradiation time similar to what was observed in samples irradiated without added MeOH (Figure 12a). The first order rate constant for the degradation (Figure 12b) was statistically equivalent (t-test, 95% confidence level) in both cases suggesting that there was no secondary reaction between the hydroxyl radicals and domoic acid.

Upon the absorption of UV radiation by dissolved organic material (DOM) in natural waters, oxygen undergoes a variety of photochemical transformations that lead to the formation of many different reactive oxygen species such as the superoxide anion and singlet oxygen (Kieber et al., 2003). Once produced, these oxygen species are reactive towards a broad range of organic species such as alkenes, sulfides, and phenols. A sample of domoic acid in WBSW was purged with nitrogen gas for 4 h in a nitrogen filled glove bag prior to irradiation to deoxygenate the sample, thereby preventing the formation of these oxygen species. After irradiating the sample for ten h, there was a loss of domoic acid with time (Figure 13a). The first order rate constant was equivalent (t-test, 95% confidence level) in the presence and absence of O₂ (Figure 13b) suggesting that the rate of photodegradation of domoic acid in seawater did not depend on the presence of O₂.

To evaluate the role of dissolved organic material in influencing domoic acid photodegradation, humic material (ca. 20 mg L⁻¹) was added to domoic acid in deionized water and irradiated under simulated sunlight for 10 h. Much of the radiation absorbed by humic material leads to the formation of excited molecules that participate in a number of reactions that accelerate the phototransformation of compounds that may

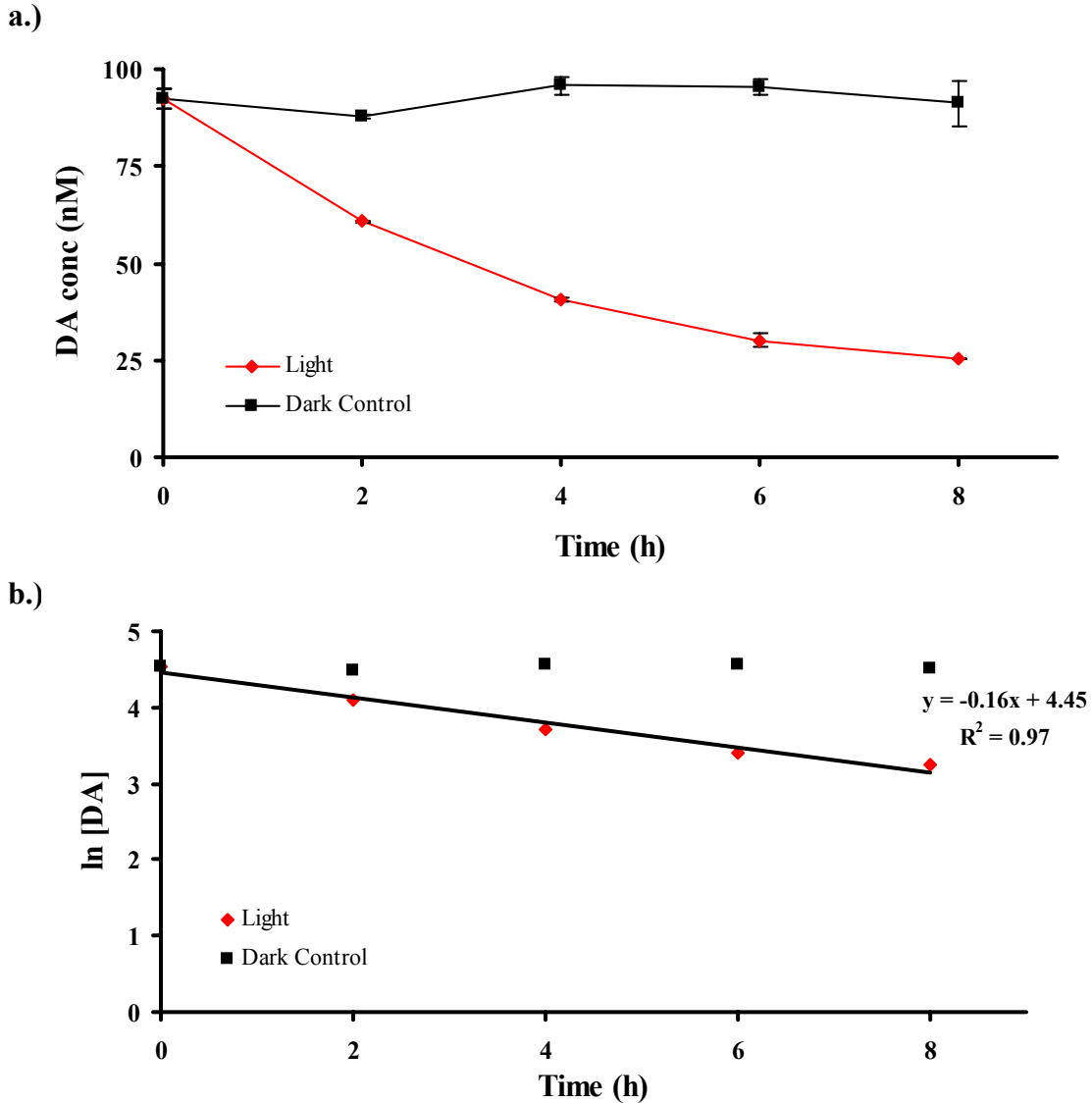


Figure 12: a) Loss of domoic acid concentration (nM) of light exposed and dark control samples as a function of irradiation time (h). The error bars represent the range ($n = 2$) while the absence of error bars signifies the range is smaller than the symbol. b) Natural logarithm of domoic acid concentration (nM) as a function of irradiation time (h). The line in the light exposed samples represents a best fit linear regression to the data. Sample consisted of domoic acid in Wrightsville Beach seawater plus 40 mM MeOH. Salinity 34; pH 8.0.

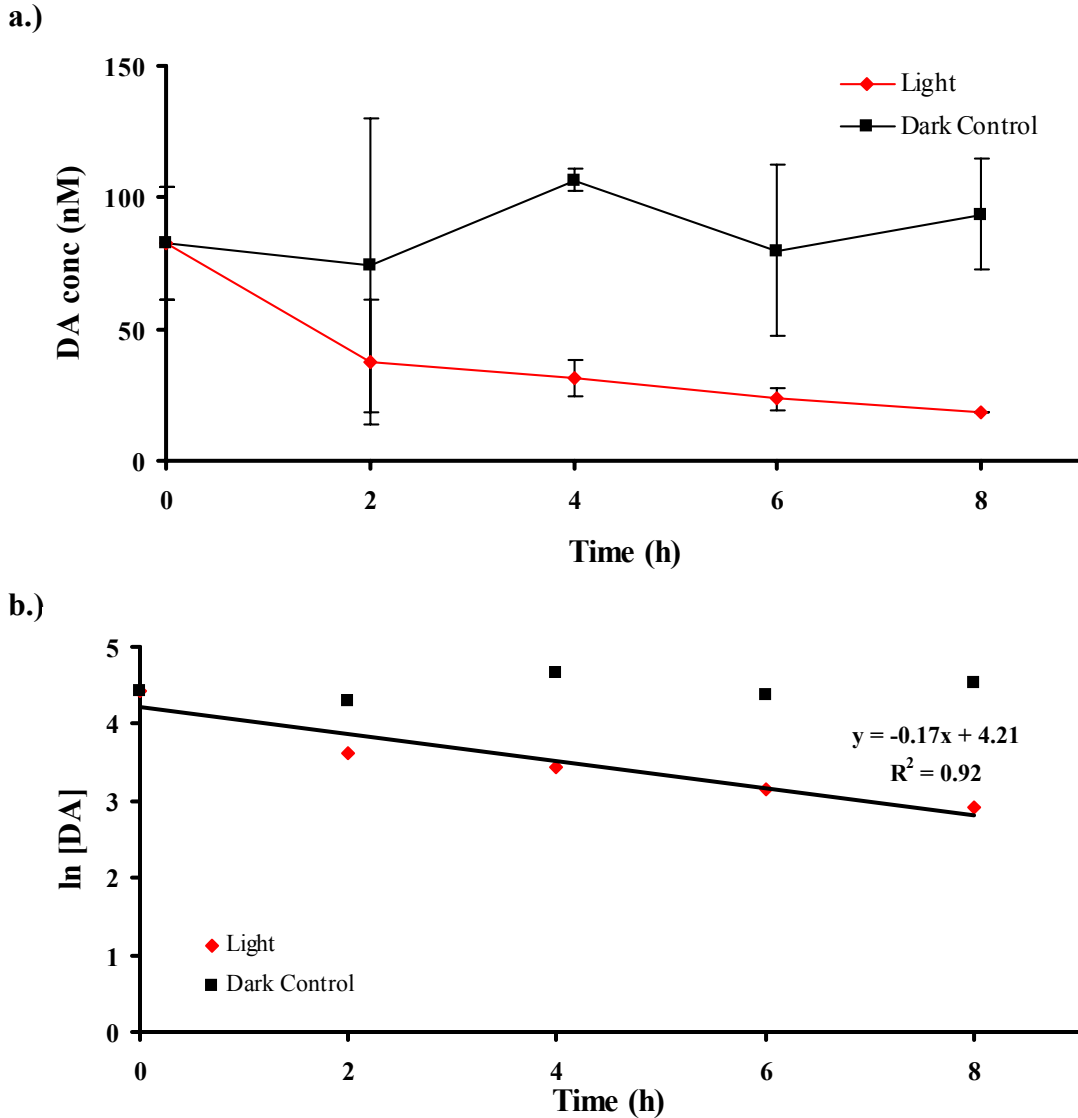


Figure 13: a) Loss of domoic acid concentration (nM) of light exposed and dark control samples as a function of irradiation time (h). The error bars represent the range ($n = 2$) while the absence of error bars signifies the range is smaller than the symbol. b) Natural logarithm of domoic acid concentration (nM) as a function of irradiation time (h). The line in the light exposed sample represents a best fit linear regression to the data. Sample consisted of 100 nM domoic acid in Wrightsville Beach seawater, and was deoxygenated with N_2 gas. Salinity 34; pH 8.4.

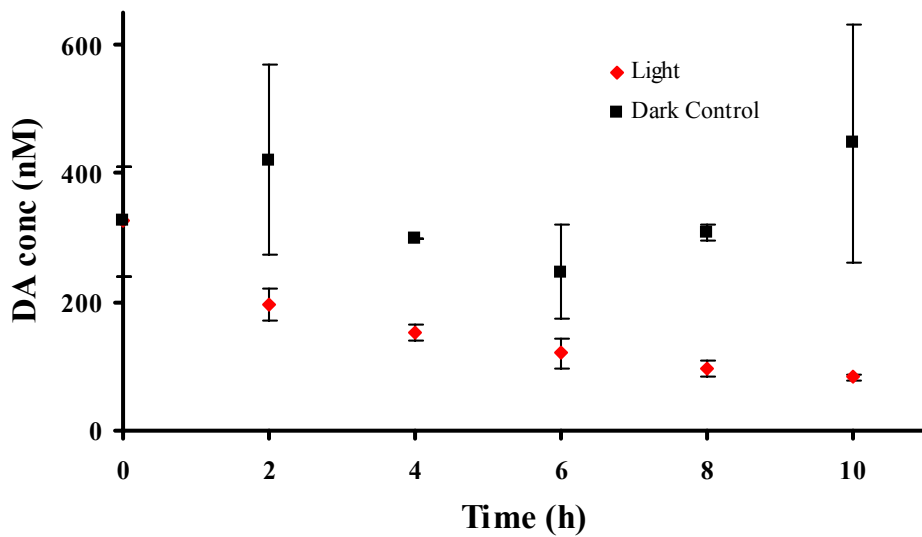
otherwise be stable (Zepp et al., 1985). The loss of domoic acid in the presence of humic material with time was similar to that observed with no added humics. The rate of degradation was statistically equivalent (t-test, 95% confidence level) with and without added humics indicating photodegradation is not dependent on the amount of humic substances present (Figure 14).

Photoproducts of Domoic Acid

Throughout the irradiation period, as the concentration of domoic acid decreased, there was an increase in the concentration of three photoproducts (Figure 15). These photoproducts have been identified as the geometrical isomers of domoic acid, isodomoic acid D, E, and F (Wright et al., 1990). A recent study by R. Bouillon (unpublished data) has found that isodomoic acid E elutes from the column at ~8.5 min, isodomoic acid F elutes from the column at ~9.0 min, and isodomoic acid D elutes from the column at ~10 min.

The isomers form within the first 2 hours of exposure to simulated sunlight. The concentration of the photoisomers was determined by assuming that the signal response of the isomers was equal to the signal response of domoic acid (Pocklington et al., 1989). In general, isodomoic acid E and D tend to form much more quickly and in higher concentrations than isodomoic acid F (Figure 16). The concentration of isodomoic acid E gradually increases until 8 h, after which its concentration no longer changes (Figure 16a). Isodomoic acid F (Figure 16b) forms much more slowly than isodomoic acid E and D, but its concentration continues to increase over the entire 10 h irradiation period. Unlike isodomoic acid E and F, the concentration of isodomoic acid D (Figure 16c)

a.)



b.)

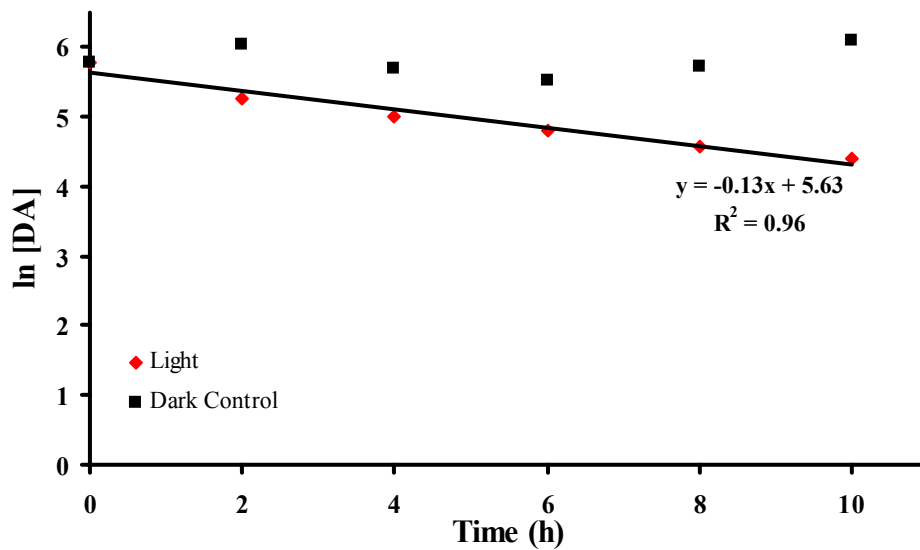


Figure 14: a) Change in domoic acid concentration (nM) in light exposed and dark control samples as a function of irradiation time (h). The error bars represent the range (n = 2) while the absence of error bars signifies the range is smaller than the symbol. b) Natural logarithm of the concentration of domoic acid (nM) as a function of irradiation time (h). The line in the light exposed sample represents a best fit linear regression to the data. Sample consists of domoic acid in deionized water with added humic material (~20 mg/mL). Salinity 0; pH 6.01.

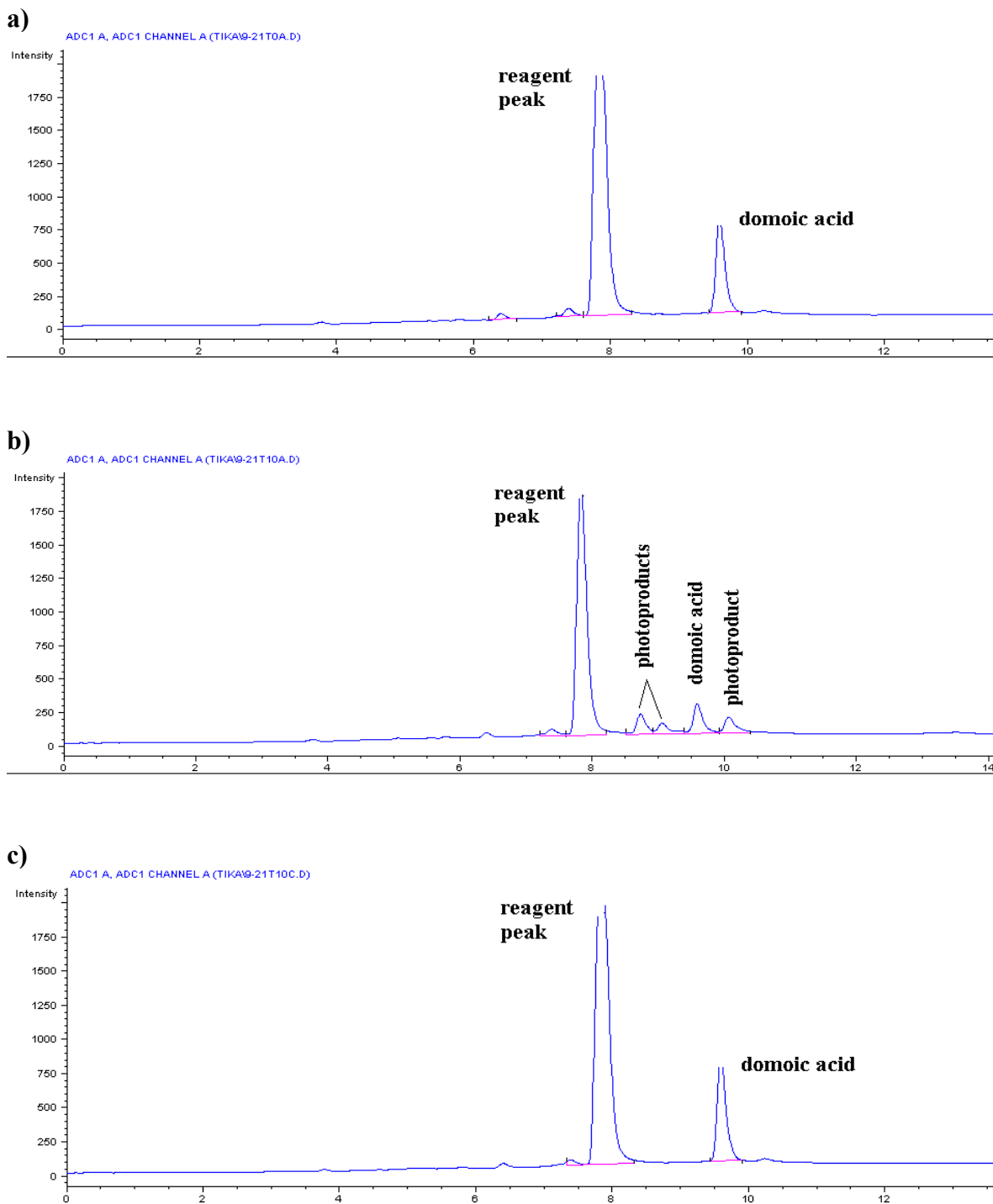


Figure 15: HPLC traces of Fmoc-derivitized domoic acid samples. a) T = 0 hours. b) light exposed sample (T = 10 h). c) dark control sample (T = 10 h). Domoic acid has a retention time of 9.5 minutes while the isodomoic acid E has a retention time of ~8.0 min, isodomoic acid F has a retention time of ~9.0 min, and isodomoic acid D has a retention time of ~10.0 min. Salinity 34; pH 8.1.

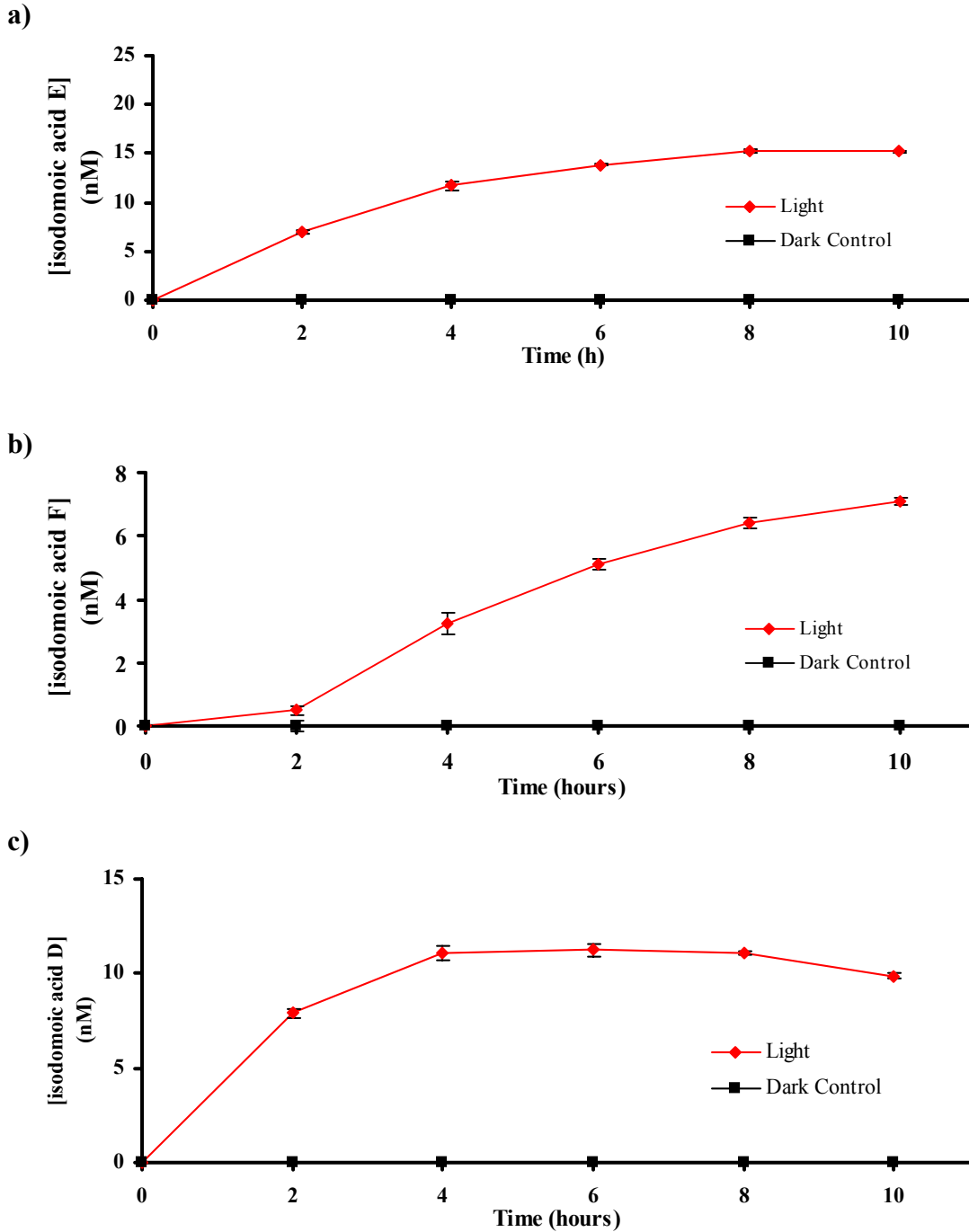


Figure 16: Concentration of domoic acid photoisomer a) E, b) F, and c) D (nM) in light exposed and dark control samples as a function of irradiation time (h) in Wrightsville Beach seawater. Error bars represent the range ($n = 2$) while the absence of error bars signifies the range is smaller than the symbol. Salinity 34; pH 8.1.

increases up until 4 h when it reaches a maximum, after which, under continued exposure to light, its concentration decreases. The concentration of each photoisomer was unchanged in the dark control samples indicating light is required for the formation of the geometrical isomers.

The same general pattern was observed in each irradiation experiment regardless of the sample matrix. This suggests that the production of the photoisomers is independent of solution composition parameters such as pH and ionic strength. Results suggest that the trace metals Fe(III) and Cu(II) may have a catalyzing effect on the production of isodomoic acid D and F (Figure 17). The production of isodomoic acid D is unaffected in the presence of Fe(III) until 6 h of irradiation, after which the rate of formation is slightly higher; however, the formation of isodomoic acid D is not significantly altered by the presence of Cu(II) (Figure 17a). The rate of formation of isodomoic acid F is significantly enhanced within the first 2-4 h of exposure to simulated sunlight when in the presence of Fe(III) and Cu(II) suggesting these trace metals may act as a catalyzing agent (Figure 17c). However, the rate of production significantly decreases after continued exposure to radiation yielding lower total concentrations of isodomoic acid F after the entire irradiation period compared to the domoic acid samples without the presence of Fe(III) or Cu(II). Unlike isodomoic acid D and F, the presence of Fe(III) and Cu(II) seem to slightly slow down the production of isodomoic acid E throughout the entire 10 h irradiation period (Figure 17b). Preliminary work indicated that all three photoisomers convert back into domoic acid under continued exposure to UV radiation (R. Bouillon, unpublished data), and an equilibrium is reached between domoic acid and the three photoisomers.

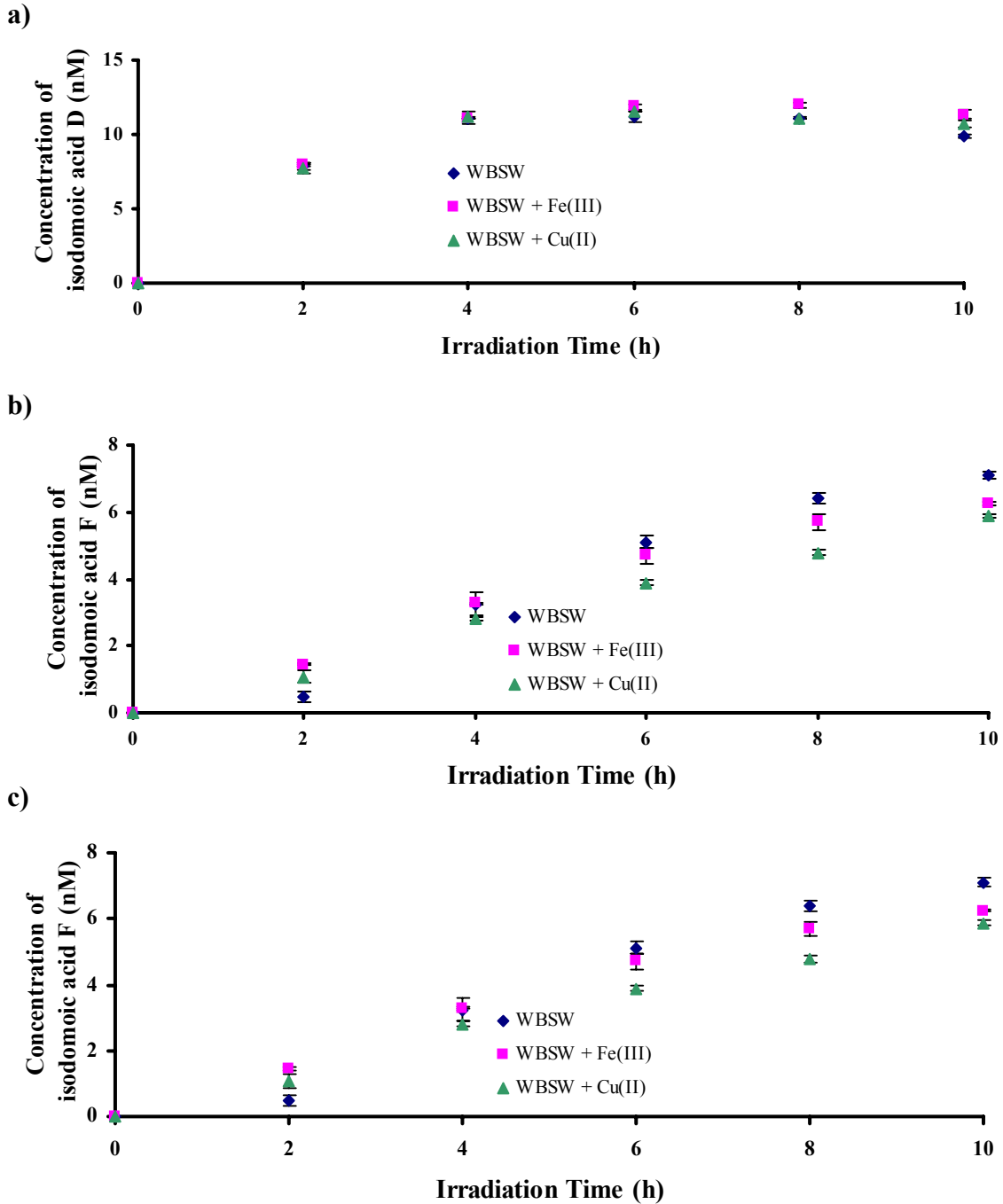


Figure 17: Comparison of the concentration (nM) of isodomoic acid a) D, b) E, and c) F as a function of irradiation time (h) for domoic acid in WBSW without added metals, domoic acid in WBSW with added Fe(III), and domoic acid in WBSW with added Cu(II).

Mechanism of Domoic Acid Photoisomerization

The lack of change in the rate of domoic acid photoisomerization regardless of sample matrix indicates that the mechanism of the photodegradation of domoic acid in seawater is a direct photochemical process, meaning domoic acid directly absorbs photons and initiates a photochemical change. The mechanism of photoisomerization of domoic acid to its geometrical isomers most likely results from the isomerization of the conjugated diene. Absorption of a photon by a compound containing a double bond often results in cis-trans geometrical isomerization (Kopecky, 1992). The absorption of a photon by a diene results in the excitation of an electron from the π (HOMO) orbital to the π^* (LUMO) orbital. Due to the high energy of the π^* MO, excitation is followed by a rapid relaxation to the geometry of the lowest energy and minimum electronic interaction (orthogonal geometry), and vibrational energy is released. There is effectively no π bond in the (π , π^*) excited state of the alkene due the large energy difference between the two states, so rotation about the σ bond produces the orthogonal geometry. Delocalization of the π electrons leads to a mixture of both cis and trans isomers (Kopecky, 1992).

There are two possible pathways for cis-trans isomerization of a conjugated diene to occur. The first involves absorption of a photon by the diene, which in turn is excited to a higher energy singlet state. Upon absorption of a photon, an electron is excited to the lowest unoccupied molecular orbital (LUMO). There is a redistribution of charges in the compound which leads to a polar structure called a zwitterion. A π bond is essentially broken which allows the molecule to twist about the sigma bond. It then returns to the ground singlet state forming either geometrical isomer. The structure of domoic acid has a side chain with Z-E geometry. The cis-trans isomers that are seen in the HPLC traces

of UV-irradiated domoic acid are thus obtained through the transition of the excited electron upon the return to ground state. A proposed mechanism for this singlet-singlet transition for domoic acid is shown in Figure 18. The second possibility involves the absorption of photons by the diene, which in turn is excited to a higher energy triplet state and the production of a biradical intermediate. Again, the π bond is essentially broken which allows the molecule to twist and form a mixture of geometrical isomers upon the return to the singlet ground state. Triplet-singlet transitions are normally forbidden due to the large singlet-triplet splitting for alkenes and dienes. However, when it does occur, intersystem crossing is usually slow and inefficient. Intersystem crossing ($S_x \rightarrow T_{x-1}$ or $T_x \rightarrow S_{x-1}$ transitions) occurs in this case due to the twisted T_1 and S_0 states being nearly equal in energy (Kopecky, 1992). A proposed mechanism for this triplet-singlet transition for domoic acid is shown in Figure 19.

The total concentration of domoic acid and the geometrical photoisomers steadily decreased in the light exposed samples (Figure 20). The total concentration of domoic acid and isomers did not change in the dark controls indicating that this loss was photochemically driven. Loss in the total domoic acid signal with time indicates another process, in addition to photoisomerization, is involved in the photochemistry of domoic acid in seawater. Earlier studies have suggested that a decarboxylated derivative of domoic acid is formed under high energy UV irradiation of domoic acid (Campbell et al., in press). It is possible the same process may account for loss of total domoic acid in simulated sunlight observed here. A proposed mechanism for the production of the decarboxylated derivative of domoic acid by Campbell et al. (in press) is shown in Figure 21.

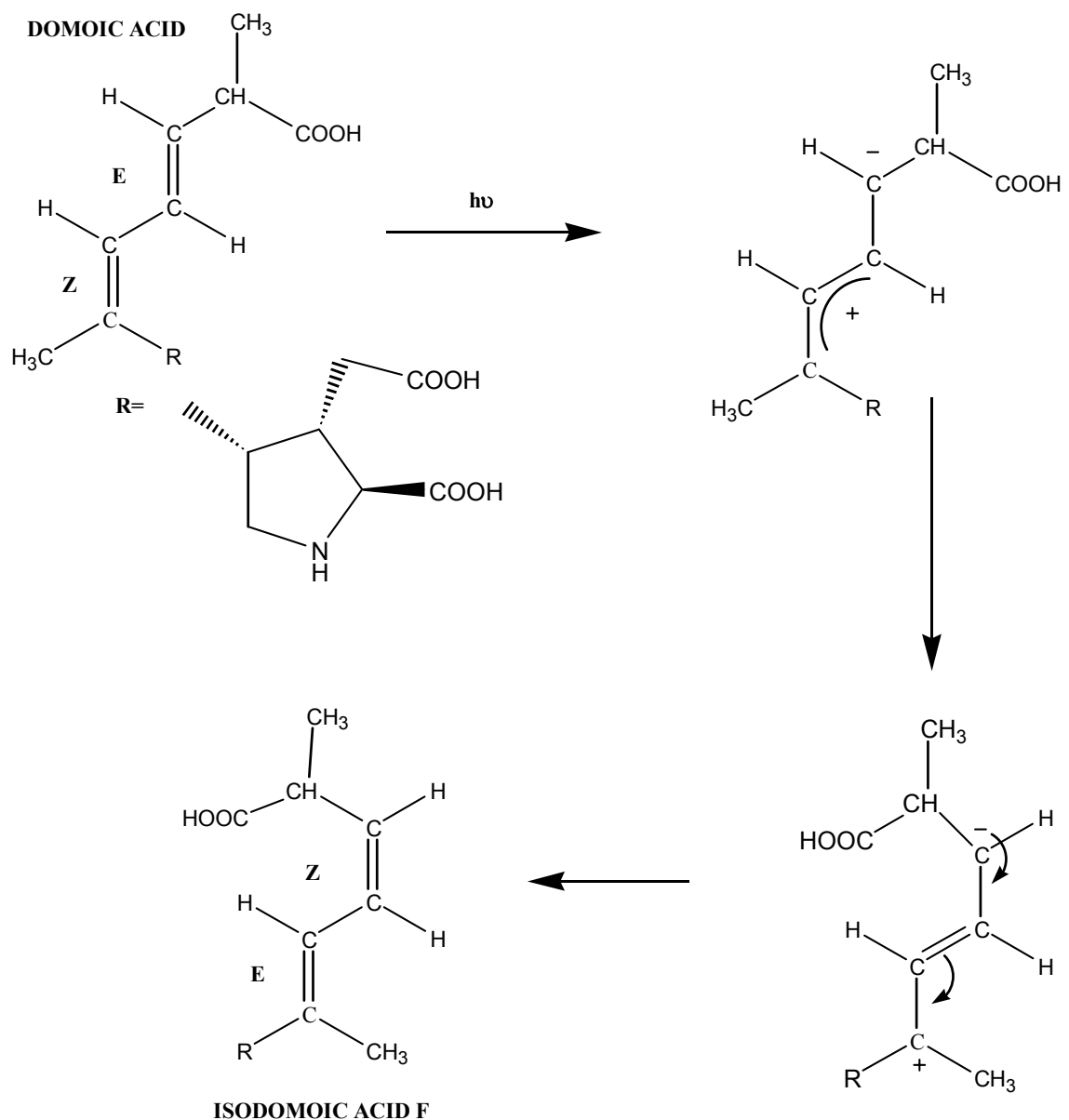


Figure 18: Proposed mechanism of photoisomerization of domoic acid to form isodomoic acid F. Upon the absorption of a photon, an electron is excited to the LUMO and a zwitterion is formed. The formation of the geometrical isomers occurs through a $S \rightarrow S$ transition once the electron returns to the singlet ground state.

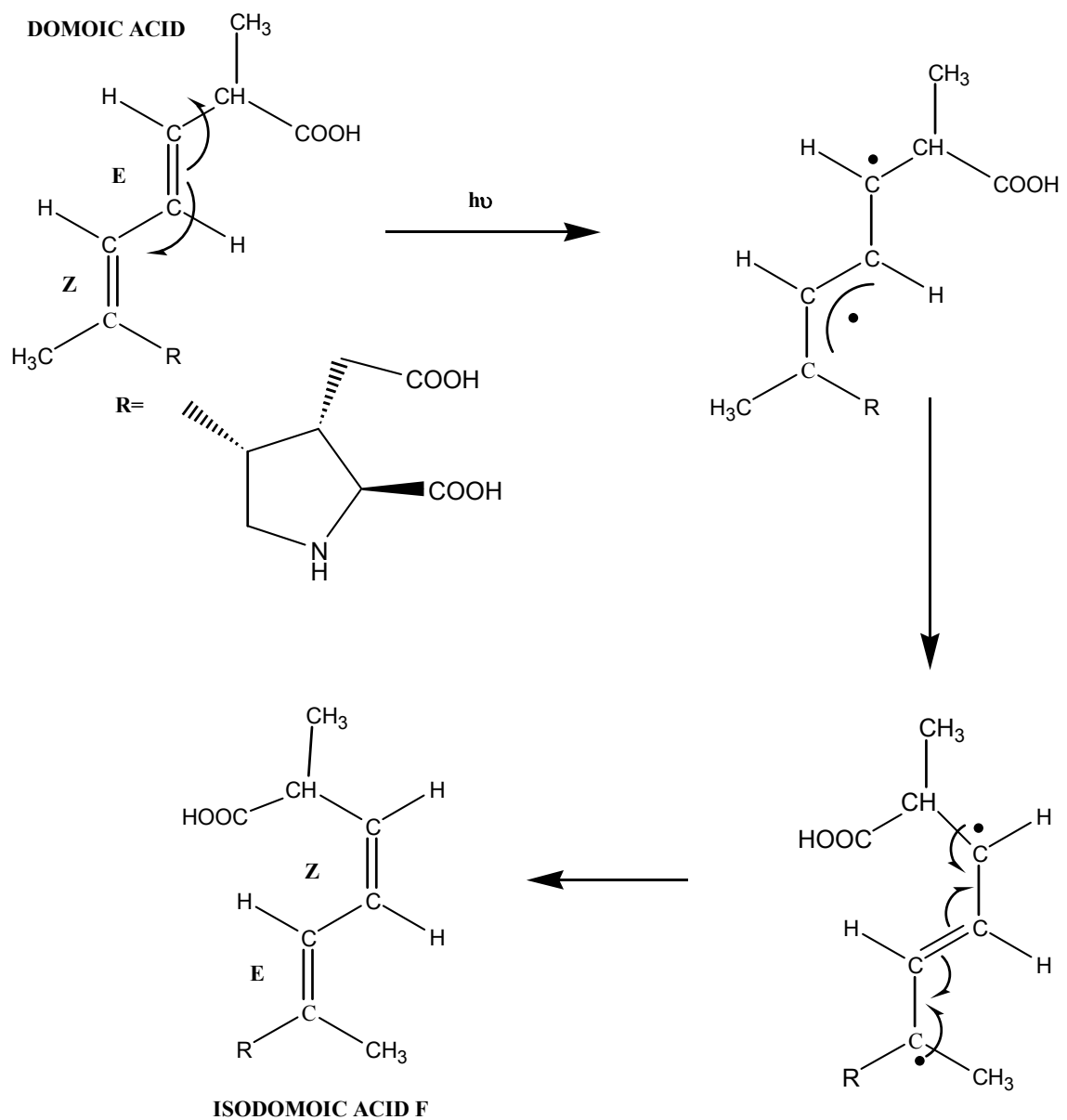


Figure 19: Proposed mechanism of photoisomerization of domoic acid to form isodomoic acid F. Upon the absorption of a photon, an electron is excited to the LUMO and a biradical is formed. The formation of the geometrical isomers occurs through a T→S transition once the electron returns to the singlet ground state.

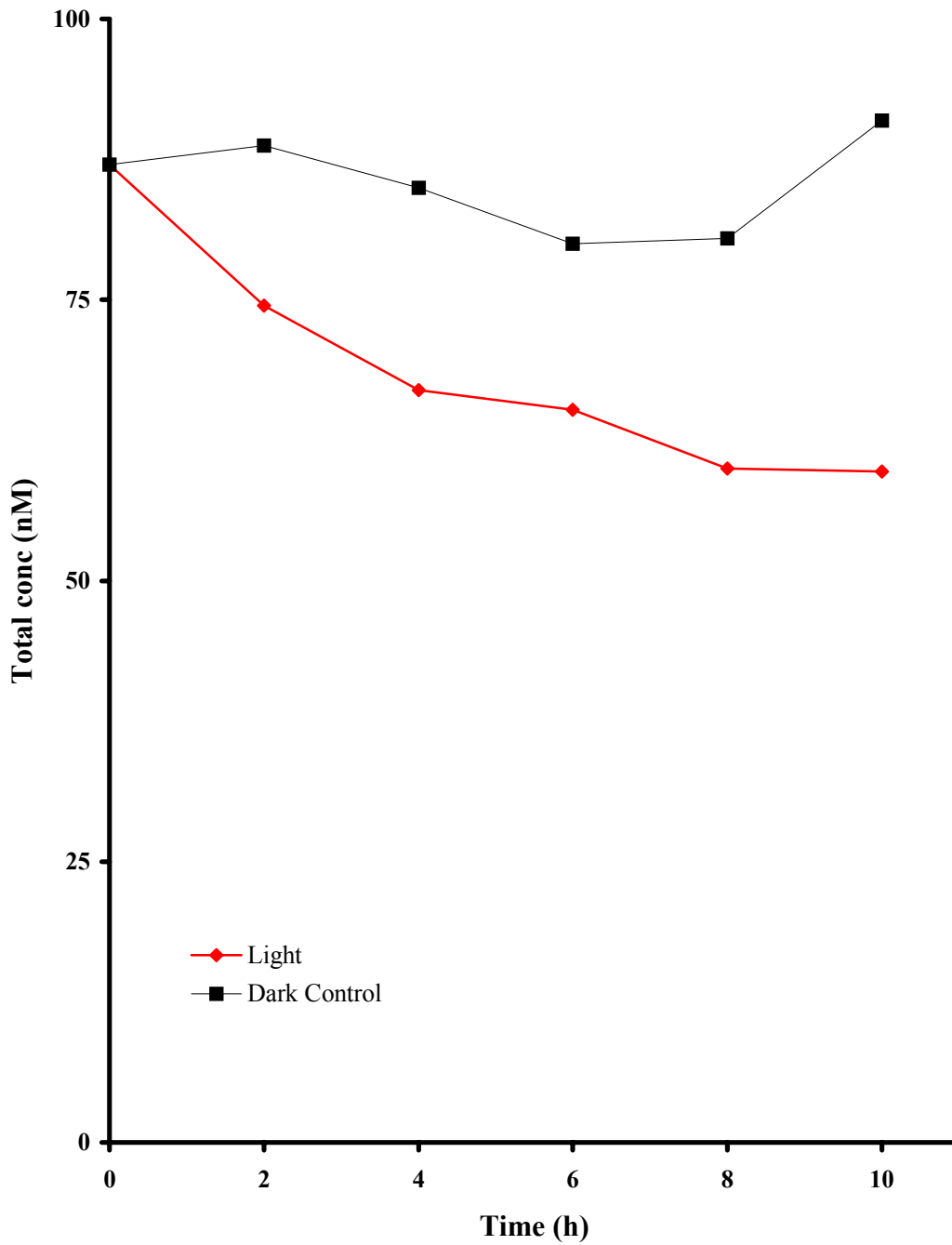


Figure 20: Total concentration of domoic acid plus photoisomers 1, 2, and 3 (nM) of light exposed and dark control samples as a function of time (h) in Wrightsville Beach seawater. Salinity 34; pH 8.0.

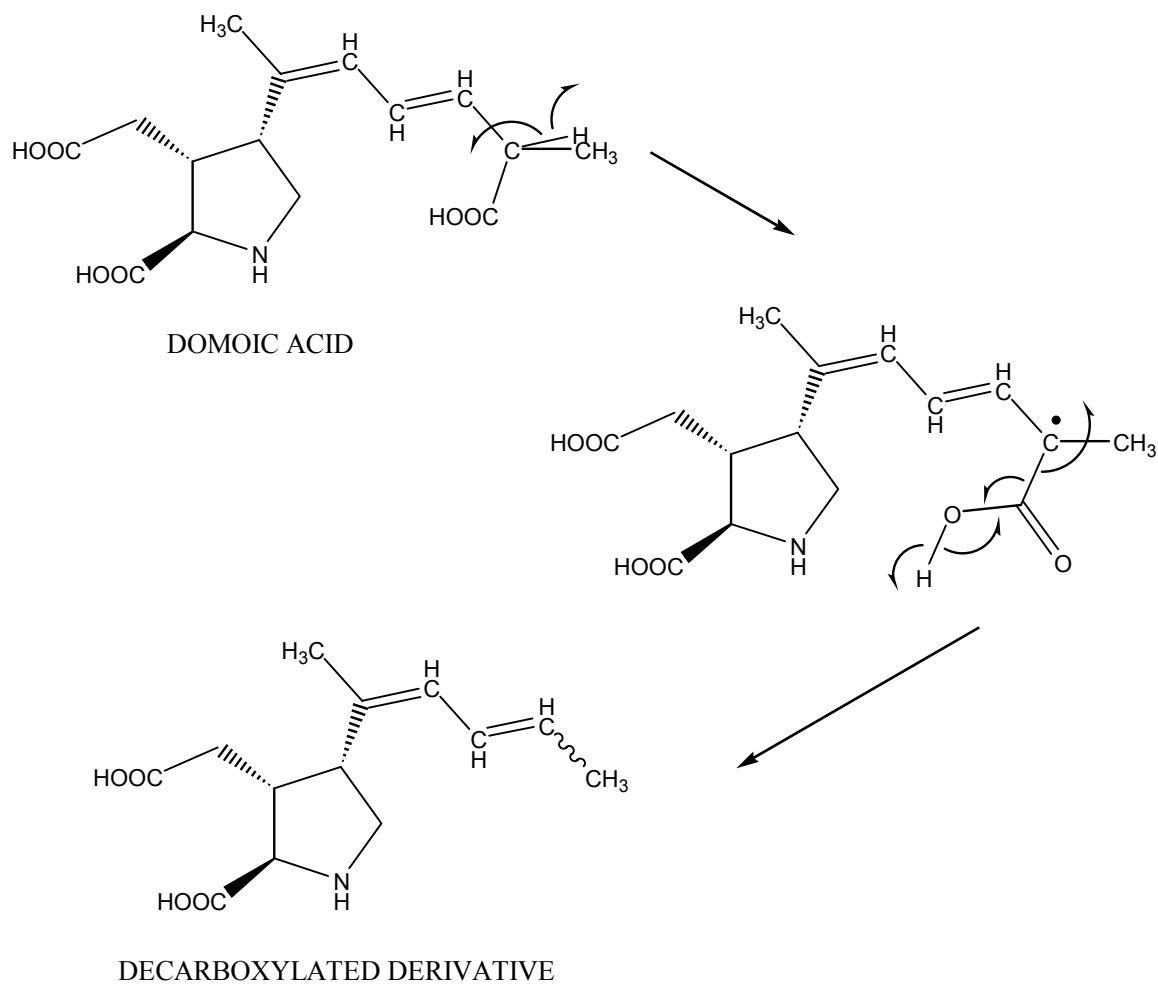


Figure 21: Proposed mechanism for the photodecarboxylation of domoic acid (Campbell et al., in press).

A comparison of the first order rate constants for the change in total domoic acid concentration (domoic acid plus photoisomers) in WBSW, WBSW with added Fe(III), and WBSW with added Cu(II) suggests the presence of Fe(III) and Cu(II) do not affect the rate of change of the total domoic acid (Figure 22). The average first order rate constant of the total domoic acid concentration in WBSW without added metals is $0.038 \pm 0.013 \text{ h}^{-1}$ while those for the addition of Fe(III) and Cu(II) are $0.045 \pm 0.013 \text{ h}^{-1}$ and $0.043 \pm 0.005 \text{ h}^{-1}$ respectively. Statistical analyses (t-test; 95% confidence level) have indicated that these values are equivalent. Given the change in total domoic acid concentrations are not affected by the presence of Fe(III) and Cu(II) and that the loss of total domoic acid is due to the formation of decarboxylated products, these results suggest the presence of trace metals such as Fe(III) and Cu(II) does not affect the rate of photodecarboxylation of domoic acid.

Activation Energy of Domoic Acid Photoisomerization in Seawater

A series of temperature studies was conducted to determine the activation energy required for the photoisomerization of domoic acid in seawater. Domoic acid was irradiated under simulated sunlight in a controlled temperature water bath at four different temperatures ($T = 5^{\circ}\text{C}$, 10°C , 15°C , and 20°C). The temperature dependence of the experimental rate data was represented by the Arrhenius equation (1):

$$k = Ae^{-\frac{E_a}{RT}} \quad (1)$$

where k is the rate constant, E_a is the activation energy, R is the gas constant ($8.314 \text{ J/mol}\cdot\text{K}$), T is the absolute temperature, and A is the frequency factor which remains constant as the temperature varies. Taking the natural logarithm of both sides of equation 1 yields:

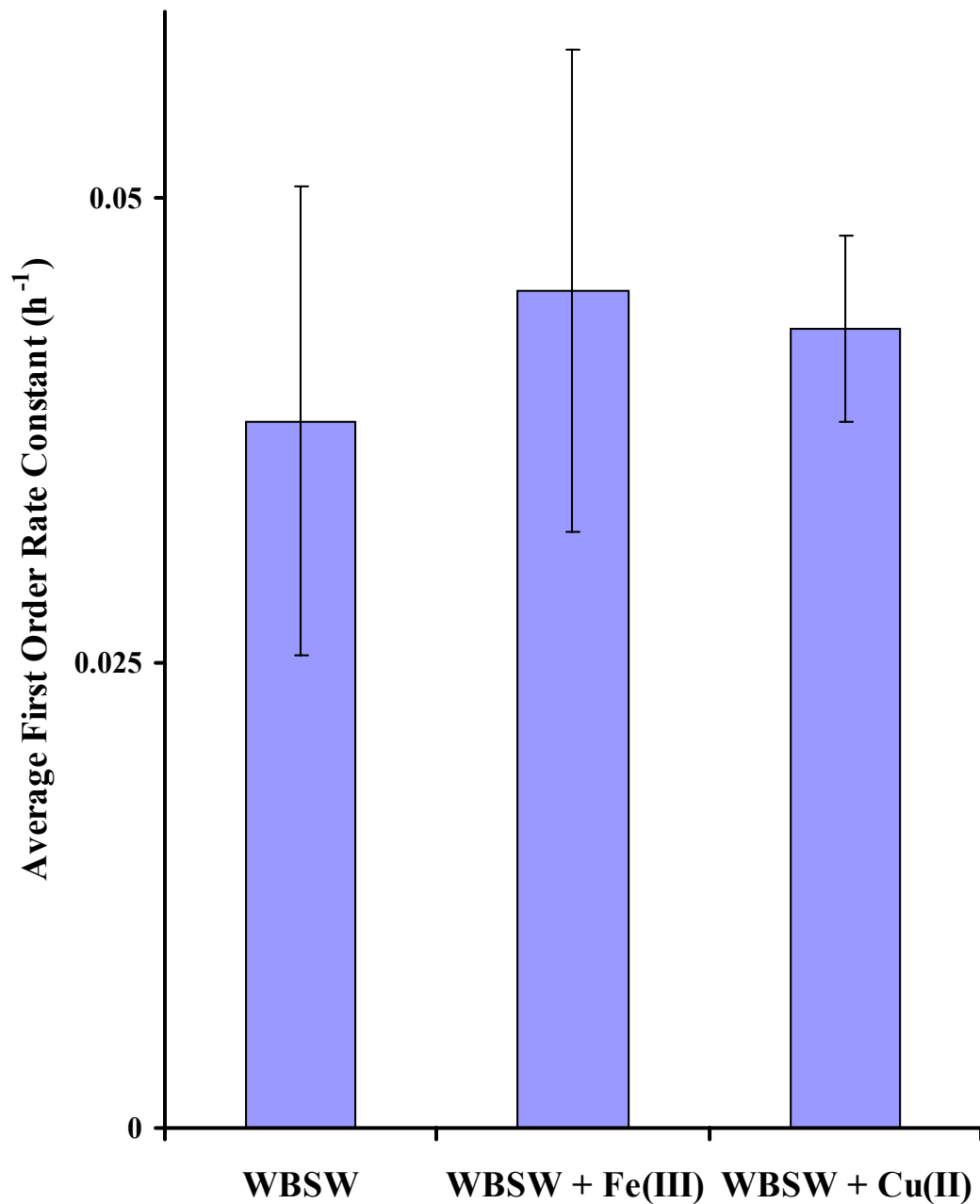


Figure 22: Average first order rate constants for the change in total domoic acid (domoic acid plus photoisomers) concentration for WBSW, WBSW plus added Fe(III), and WBSW plus added Cu(II). The error bars represent the standard deviation (n = 4).

$$\ln k = -\frac{E_a}{RT} + \ln A \quad (2)$$

The natural logarithm of the resulting first order rate constants were plotted as a function of the reciprocal of the incubation temperature (Figure 23). The rate of photodegradation of domoic acid decreased as the temperature decreased. The activation energy was calculated from the slope of the resulting line and was determined to be 13 kJ mol⁻¹.

Quantum Yield Studies

A series of controlled photolysis studies was conducted to determine which wavelengths in the solar spectrum are most efficient at the photodegradation of domoic acid in seawater. Significant loss of domoic acid was observed within the first 2 h of exposure to full spectrum simulated sunlight with as much as 75% lost in 10 h of exposure. When ultraviolet radiation (280 nm – 400 nm) was removed during irradiation of the sample, there was no loss of domoic acid in light exposed samples (Figure 24) indicating that ultraviolet radiation is responsible for the photochemically-induced activity of domoic acid.

A second series of experiments was conducted with monochromatic irradiation rather than simulated sunlight in order to determine the quantum yield of domoic acid photodegradation (R. Bouillon, unpublished data). The efficiency of a photoprocess is measured in terms of its quantum yield (Φ) where Φ is equal to the moles of product formed (or reactants lost) per mole of photons absorbed by the analyte. The sum of the quantum yields of all primary processes occurring within an irradiated system is equal to one while Φ is equal to zero when there is no reaction.

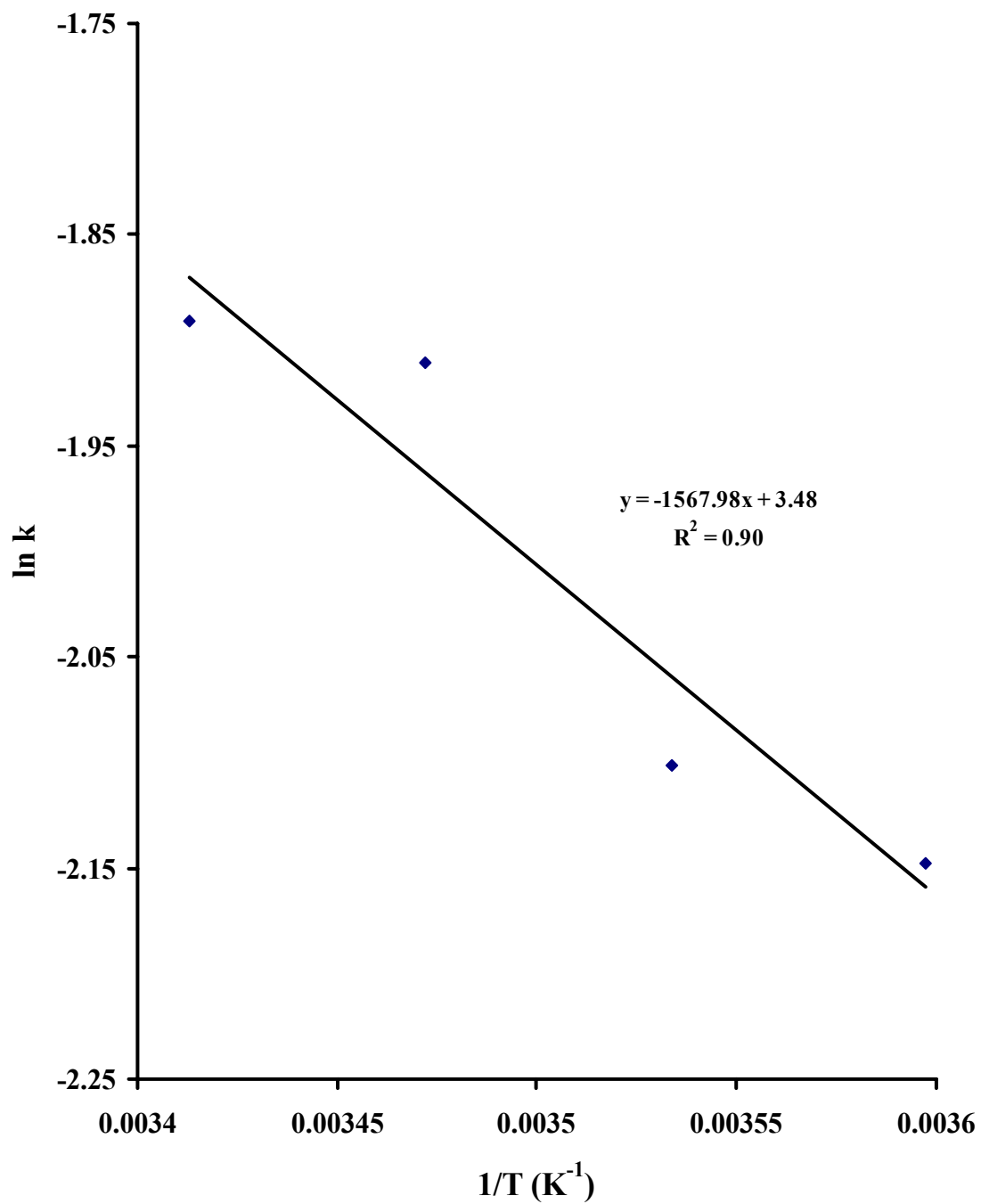


Figure 23: Natural logarithm of the first order rate constant of photodegradation of domoic acid in Wrightsville Beach seawater as a function of the reciprocal of the incubation temperature (K⁻¹).

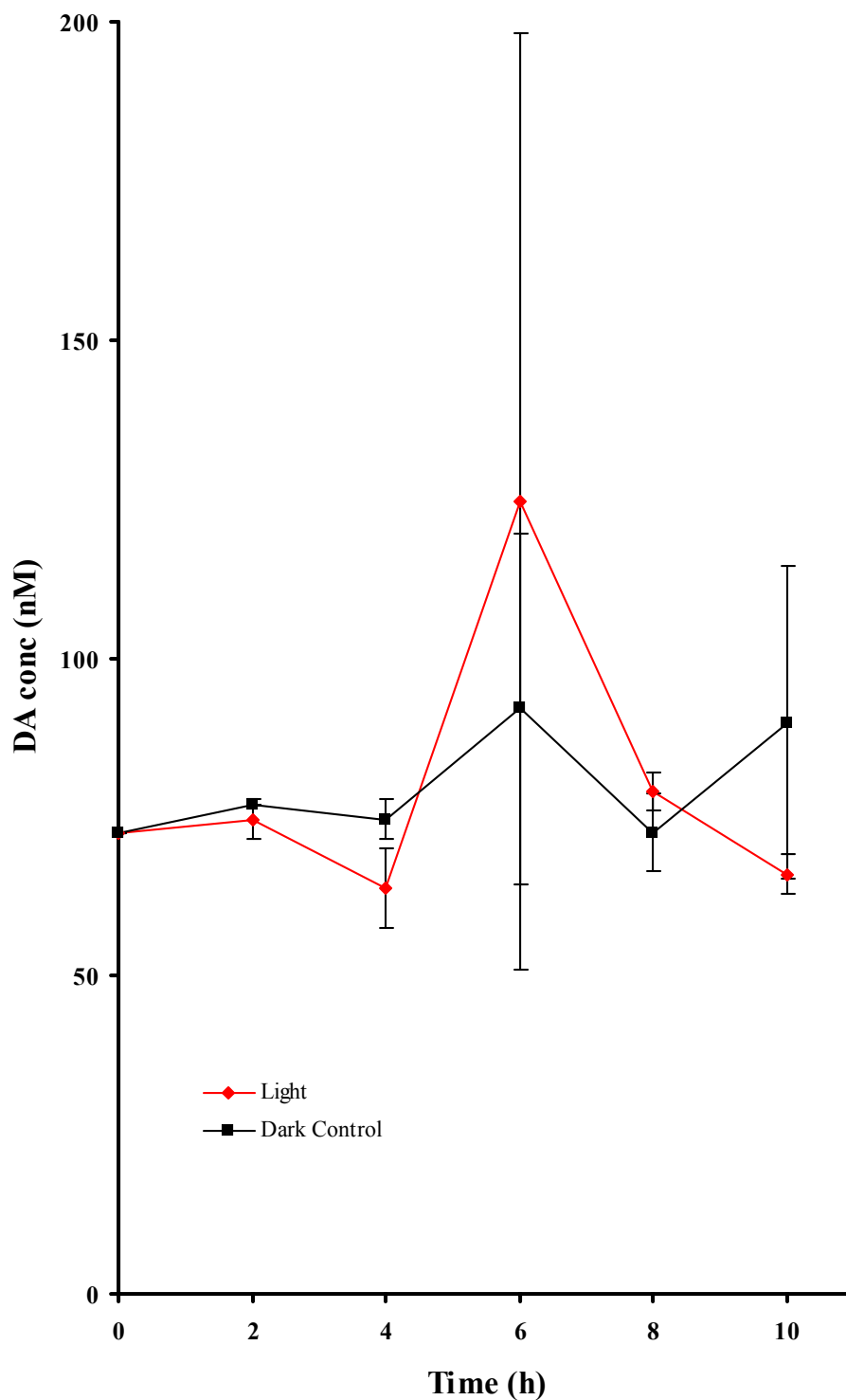


Figure 24: Concentration of domoic acid (nM) in light exposed and dark control samples as a function of irradiation time (h) in deionized water. Sample was exposed to UV wavelengths (280 – 400 nm) only. Error bars represent the range (n = 2) while the absence of error bars signifies the range is smaller than the symbol. Salinity 0; pH 5.9.

Evidence suggests domoic acid undergoes direct photochemical degradation.

Given this, the degradation rate of domoic acid due to direct irradiation in an optically thin solution is defined as (Zepp, 1977):

$$-\frac{d[DA]}{dt} = 2.303 [DA] \int E_0(\lambda) \Phi_{DA}(\lambda) \left(\frac{area}{volume} \right) \varepsilon(\lambda) l \quad (3)$$

where $-\frac{d[DA]}{dt}$ is the rate of change of DA concentration with time in mol DA L⁻¹ s⁻¹,

[DA] is the domoic acid concentration in mol L⁻¹, $E_0(\lambda)$ is the incident spectral irradiance in mol photons cm⁻² s⁻¹ nm⁻¹, area is the surface area irradiated in cm², volume is the volume of water being irradiated in cm³, $\Phi_{DA}(\lambda)$ is the quantum yield in

$\frac{mol\ DA\ lost}{mol\ photons\ absorbed}$, $\varepsilon(\lambda)$ is the molar absorption coefficient of domoic acid in L

mole⁻¹ cm⁻¹, and l is the irradiation pathlength or depth in cm (Whitehead and de Mora, 2000).

Integration of equation 3 under the boundary conditions ($t = 0$, [DA]₀) and (t , [DA]_t) yields

$$-\frac{\ln[DA]_t}{[DA]_0} = 2.303 E_0(\lambda) \Phi_{DA}(\lambda) \left(\frac{area}{volume} \right) \varepsilon(\lambda) l \quad (4)$$

and rearrangement of equation 4 gives a quantum yield that is equal to

$$\Phi_{DA}(\lambda) = \frac{-(\ln[DA]_t / [DA]_0) / t}{E_0(\lambda) (area / volume) \varepsilon(\lambda) l} \quad (5)$$

An efficiency spectrum, defined as quantum yield as a function of irradiation wavelength, was produced using equation 5 to determine the efficiency of specific

wavelengths that results in photoisomerization of domoic acid. The efficiency spectrum was generated by plotting the quantum yield of domoic acid in deionized water as a function of wavelength (Figure 25). The data was interpolated in order to estimate quantum yields at all wavelengths. The efficiency of domoic acid photodegradation rapidly decreases as the irradiance wavelength increases, particularly between 280 and 315 nm. There is a slight increase in the efficiency of degradation from 315 nm to 335 nm, but beyond 335 nm the efficiency of photodegradation drops off rapidly. This is most likely because the energy of the incoming radiation decreases with higher wavelengths.

The efficiency spectrum was multiplied by the absorbed dose rate (wavelength local actinic flux multiplied by the average absorbance spectrum) to develop a wavelength dependent response spectrum (Figure 26). The response function is given in units of moles L⁻¹ day⁻¹. The rate of photoisomerization was fastest at wavelengths ranging from 330 nm to 350 nm suggesting that these wavelengths are most efficient at inducing photochemical changes of domoic acid in seawater.

The photodegradation of domoic acid in natural waters is much more complex than the scenario stated above. During bloom events, it is necessary to know the area and depth in which the domoic acid is present in order to accurately calculate a response spectrum of domoic acid. In natural seawater, the rate of photodegradation of a substance, in this case domoic acid, is given by (Whitehead and de Mora, 2000):

$$-\frac{d[DA]}{dt} = 2.303[DA] \int E(\lambda) \Phi(\lambda) \varepsilon(\lambda) d\lambda \quad (6)$$

Equation 6 does not take into account the area of water being irradiated and is a generalization for surface waters.

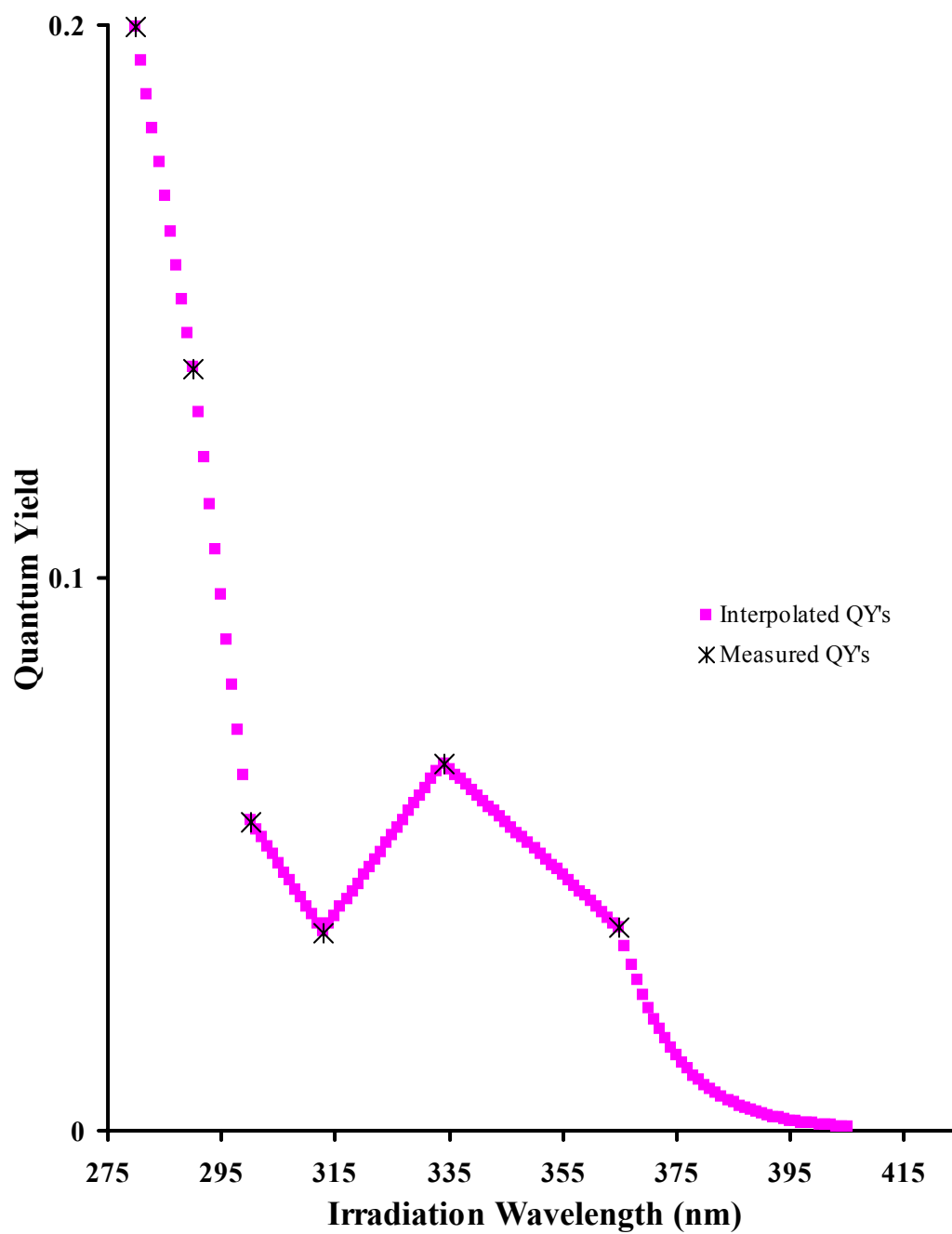


Figure 25: Quantum yield (moles of DA lost / mole of photons absorbed) as a function of irradiation wavelength (nm).

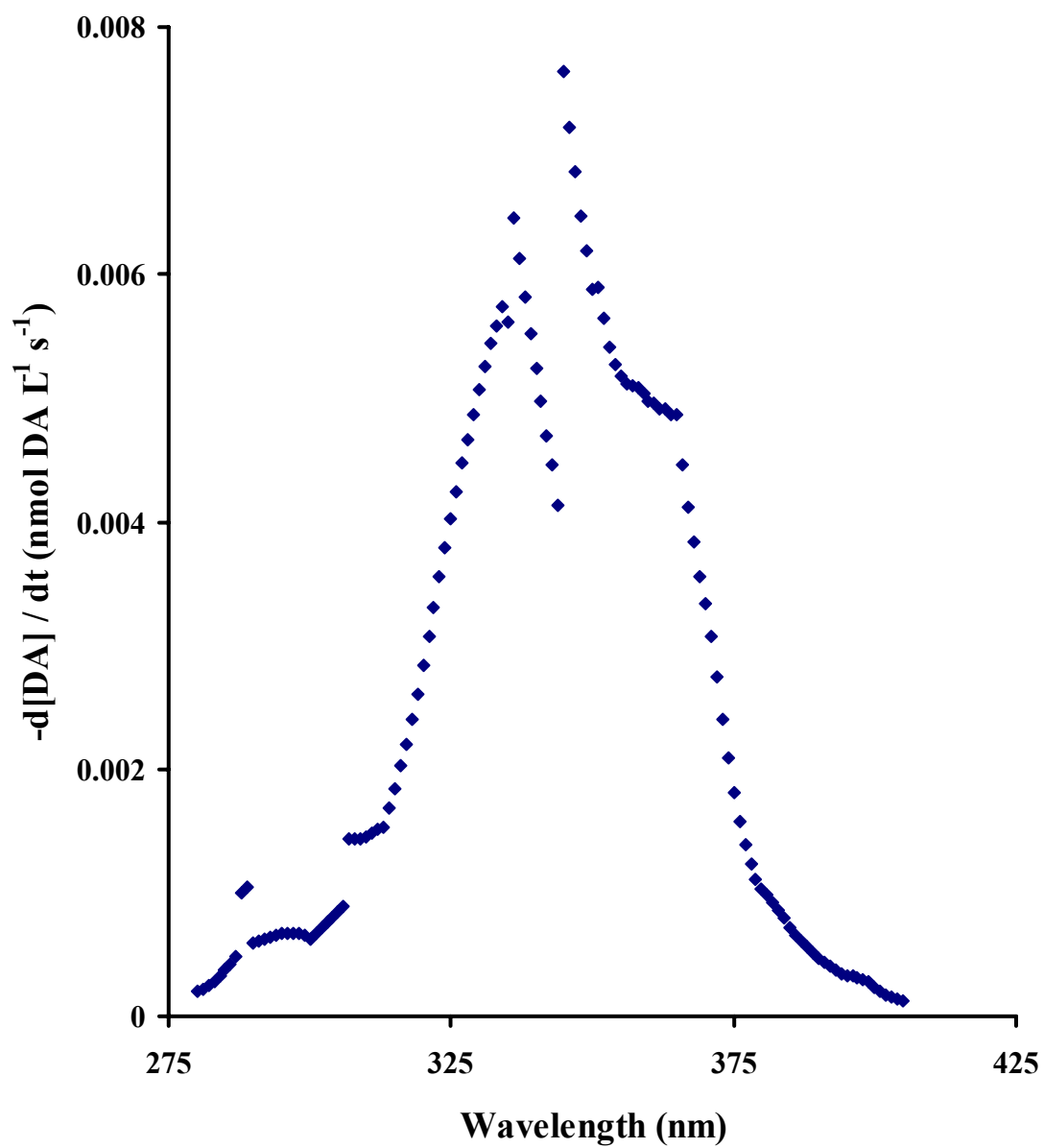


Figure 26: The rate of change of domoic acid concentration over time as a function of irradiation wavelength (nm).

The quantum yield values of domoic acid photoisomerization are comparable to those for other direct photoprocesses. Hydroxyl radical production from nitrate and nitrite photolysis are well-known direct photochemical processes. The quantum yield of domoic acid photoisomerization is roughly 2-3 times that for the hydroxyl production from nitrate photolysis at any given wavelength and roughly equal to that for the hydroxyl production from nitrite photolysis (Jankowski et al., 1999).

The production of Fe(II) in rainwater at lower wavelengths is similar to dissolved inorganic carbon (DIC) production in lakes, coastal waters, and open ocean waters which is an indirect photochemical process (Hardison, 2002). The quantum yield values for dissolved inorganic carbon in lakes, coastal waters, and open ocean waters are 1-2 orders of magnitude less than those for domoic acid photoisomerization at any given wavelength. Indirect photochemical processes have much lower quantum yield values indicating a much less efficient reaction.

CONCLUSIONS

Domoic acid had been found to photoconvert to a series of three geometrical isomers via the photoisomerization of the conjugated diene. This photoisomerization is not significantly affected by factors such as DOC, pH, ionic strength, or the presence of hydroxyl radicals or reactive oxygen species suggesting that this photoisomerization is a direct photochemical process. Likewise, the presence of trace metals such as Fe(III) and Cu(II) do not affect the rate of photoisomerization of domoic acid; however, they seem to play some role in the production of decarboxylated derivatives of domoic acid.

Quantum yield studies have indicated that domoic acid undergoes photoisomerization most efficiently when subjected to UV radiation, specifically

wavelengths ranging from 330-350 nm. These results can be applied to real-world toxic bloom events that occur throughout our coastal waters to obtain a better understanding of the role played by domoic acid in the water column. Using the results gained from this research, it is possible to model the behavior of dissolved domoic acid produced by a toxic bloom of *Pseudo-nitzschia*. By knowing the quantum yield and absorbance spectrum of domoic acid, as well as the solar irradiance data and the optical properties of the body of water, modeling studies may be done to determine the residence time of domoic acid in the water column during a toxic bloom event.

Future research on the photochemistry of domoic acid in natural waters will focus on determining more accurate values for the quantum yield and response spectrum of domoic acid photoisomerization in seawater. This would be helpful in the modeling of domoic acid in natural waters. Additional research will be conducted to determine the toxicity of the photoproducts, both photoisomers and the decarboxylated derivatives of domoic acid. Field work will also be performed during bloom events off the coast of eastern Canada and northern California in hopes of modeling the lifetime of domoic acid under ambient conditions in the water column.